Population Exposure to Compound Precipitation–Temperature Extremes in the Past and Future Climate across India

SUBHASMITA DASH,[a] RAJIB MAITY,[a,b] AND HARALD KUNSTMANN[b,c,d]

[a] *Department of Civil Engineering, Indian Institute of Technology Kharagpur, Kharagpur, West Bengal, India*
[b] *Institute of Meteorology and Climate Research (IMK-IFU), Karlsruhe Institute of Technology, Garmisch-Partenkirchen, Germany*
[c] *Institute of Geography, University of Augsburg, Augsburg, Germany*
[d] *Center for Climate Resilience, University of Augsburg, Augsburg, Germany*

(Manuscript received 23 December 2022, in final form 11 October 2023, accepted 16 October 2023)

ABSTRACT: This study explores the population exposure to an increasing number of hydroclimatic extreme events owing to the warming climate. It is well agreed that the extreme events are increasing in terms of frequency as well as intensity due to climate change and that the exposure to compound extreme events (concurrent occurrence of two or more extreme phenomena) affects population, ecosystems, and a variety of socioeconomic aspects more adversely. Specifically, the compound precipitation–temperature extremes (hot-dry and hot-wet) are considered, and the entire Indian mainland is regarded as the study region that spans over a wide variety of climatic regimes and wide variation of population density. The developed copula-based statistical method evaluates the change in population exposure to the compound extremes across the past (1981–2020) and future (near future: 2021–60 and far future: 2061–2100) due to climate change. The results indicate an increase of more than 10 million person-year exposure from the compound extremes across many regions of the country, considering both near and far future periods. Densely populated regions have experienced more significant changes in hot-wet extremes as compared with the hot-dry extremes in the past, and the same is projected to continue in the future. The increase is as much as sixfold in many parts of the country, including the Indo-Gangetic Plain and southernmost coastal regions, identified as the future hotspots with the maximum increase in exposure under all the projected warming and population scenarios. The study helps to identify the regions that may need greater attention based on the risks of population exposure to compound extremes in a warmer future.

SIGNIFICANCE STATEMENT: How is the growing population being affected now, and in the future, how will it be affected due to climate change induced compound extreme events? This study explores this societal consequence in terms of population exposure for the most populous country, India. An increase of more than 10 million person-year exposure from the precipitation–temperature compound extremes across many regions is indicated. Densely populated regions are expected to experience enhanced population exposure to hot-wet extremes as compared with the hot-dry extremes. Furthermore, the maximum increase in population exposure to compound extremes is expected across the Indo-Gangetic Plain and southern coastal regions of India. The outcome of the study will be helpful for adopting socioeconomic decisions toward the welfare of society.

KEYWORDS: Extreme events; Precipitation; Climate change; Temperature; Societal impacts

1. Introduction

Climate change, as defined by the Intergovernmental Panel on Climate Change (IPCC), refers to the long-term alterations in climate (Pielke 2005) caused by various factors that affect the atmosphere's radiative properties and global energy balance, such as greenhouse gas emission, solar radiation changes, volcanic emission, and aerosols (Adedeji et al. 2014; Shen et al. 2020). Climate change has exacerbated extreme climate phenomena. As a result, the recent decades have witnessed more frequent and intensified wet and dry extremes (Breinl et al. 2020; Stevenson et al. 2022; Labonte and Merlis 2023). Both wet and dry extremes pose huge pressure on natural and human systems in terms of water availability and management. Furthermore, dry extremes are expected to become spatially more extensive and prolonged in the future, while amplification of extreme wet precipitation has also been projected (Myhre et al. 2019; De Luca et al. 2020) on global scales. Alongside this, increasing population exposure to extreme temperature conditions is evidenced worldwide (Rogers et al. 2021). More importantly, under the potential future warming, heat extremes are anticipated to become severe, further increasing the heat related morbidity and mortality rates, specifically in developing low-latitude countries like India (Mazdiyasni et al. 2017; Mukherjee and Mishra 2018; Li et al. 2021; Yaduvanshi et al. 2021; Yang et al. 2021).

Climate change risks related to hydroclimate extremes are influenced by two factors: changing characteristics of the extremes and the extent of societal exposure to these extremes (Jones et al. 2015). Exposure to such extremes affects the population, ecosystems, and other socioeconomic aspects that may face potential losses. India is a country with the largest

Supplemental information related to this paper is available at the Journals Online website: https://doi.org/10.1175/JHM-D-22-0238.s1.

Corresponding author: Rajib Maity, rajib@civil.iitkgp.ac.in; rajibmaity@gmail.com

DOI: 10.1175/JHM-D-22-0238.1

population in the world (Sara et al. 2023). It is also the sixth most vulnerable country to climate extremes (Mall et al. 2019). The livelihood of a major proportion of the working population is primarily dependent on agriculture. As the major proportion of the total agricultural land across the country is rain-fed, prolonged dry spells substantially affect agricultural activities (Bandyopadhyay et al. 2016; Mishra et al. 2020). Furthermore, agricultural products account for approximately 70% of India's exports, and dry extremes can have an influence on the Indian economy as well as national and global food security (Singh et al. 2014). Similarly, extremely wet conditions within a short time span can have large humanitarian impacts, such as loss of lives, water-related diseases, and loss of property (Breinl et al. 2020; Kansal and Singh 2022). Since the beginning of the twenty-first century, India has witnessed more frequent dry and wet extremes due to an erratic spatiotemporal precipitation pattern (Dash and Maity 2019; Sarkar and Maity 2020). Some of the recent devastating heavy precipitation events across different regions of the country include Mumbai (2005), Uttarakhand (2013), Chennai (2015), Gujarat (2017), Kerala (2018), Maharashtra (2019), Assam (2020), and Bihar (2020) (Ray et al. 2019). Further, floods translated through the intense precipitation events during the past two decades have severely impacted various aspects of the socioeconomic systems with about 30 000 lives lost (CRED 2023; Fig. S1a in the online supplemental material). Likewise, the country has experienced more frequent prolonged dry spells in the recent past (Mishra and Liu 2014; Singh et al. 2014) and some of the deadliest droughts affecting more than 500 million people (Fig. S1c). Moreover, the changing characteristics of dry and wet extremes can pose serious challenges toward the socioeconomic conditions, including future water availability and food security of more than 1.4 billion people (Kumar et al. 2018; Varga 2021).

Apart from the changing nature of the precipitation extremes, India has been experiencing notably warmer climate conditions since the 1980s, with each successive decade being warmer as compared with the previous ones (WMO 2020). The heat extremes can affect society and ecosystems in multiple ways, e.g., decreased air quality, increased energy consumption, higher evapotranspiration, reduced agricultural yields, and the most concerning of all, direct effects on human health (Gupta and Guleria 2017; Zhang et al. 2018). Heat stress during high temperatures may cause cardiovascular and respiratory diseases, resulting in life-threatening crises (Pradhan et al. 2019). Intensified extreme temperature conditions in the recent two decades (Pai et al. 2013; Singh et al. 2021) have resulted in around 10 000 human fatalities across India (Fig. S1b). For instance, heatwaves in 1998, 2013, and 2015 resulted in the loss of more than 2600, 1500, and 2500 people, respectively (Mishra et al. 2022).

Managing the impacts of frequent climate extremes becomes more challenging owing to rapid urbanization in developing countries like India (Avashia et al. 2021; Ridha et al. 2022; Ganguli 2023). Considering the temperature extremes, health-related heat impacts are more severe in urban areas. The reasons include the explosive growth of urban population and exposure to higher and nighttime sustained temperatures due to the urban heat island (UHI) phenomena, characterized by the rapid expansion of more heat absorbing artificial surfaces (e.g., buildings and roads) (Gao et al. 2019; Tuholske et al. 2021). For instance, heatwaves in the city of Ahmedabad in the year 2010 resulted in 1300 deaths (Knowlton et al. 2014). Furthermore, considering rising water demand, urban India is more likely to experience severe water scarcity in the future due to the growing population, associated increase in socioeconomic activities and climate change (Schewe et al. 2014). Likewise, urban regions in India are experiencing recurrent instances of short-duration wet extremes (Ali and Mishra 2018). These occurrences can result in flash floods, landslides, water-logging, and other socioeconomic consequences (Lane et al. 2013; Roderick and Wasko 2020). For instance, extreme precipitation in Mumbai in 2005 posed considerable socioeconomic impacts, including 1095 deaths (Mukherjee et al. 2018).

Consequently, the exposure from the concurrence of these temperature and precipitation extremes can more adversely affect society than their occurrence in isolation. Compound extremes are defined as (i) the simultaneous or successive occurrence of multiple extreme events, (ii) the combination of extreme events resulting in amplifying their individual impacts, or (iii) the combination of nonextreme events resulting in an extreme impact when combined (Seneviratne et al. 2012). Compound extremes in general refer to the combination of multiple extremes contributing to larger societal and environmental risk (Zscheischler et al. 2018). The compound extremes may be induced due to a common external forcing or mutual reinforcement of two extremes or when one extreme is dependent on the occurrence of another extreme. Noting the exacerbating regional warming conditions across India and the existing interdependence between precipitation and temperature (Hao et al. 2019; Sharma and Mujumdar 2019; Dash and Maity 2023), assessment based on their univariate extremes separately may undermine the risk of compound extremes (Hu et al. 2023). For instance, droughts induced through the combined effect of extreme dry spells and extreme heat conditions are notably more severe and can cause greater damage to human health, agricultural productivity, and water availability (Raza et al. 2019; Yin et al. 2022). In India, most of the regions experience extreme temperature conditions during summer (March–May). The extreme heat conditions may last longer than usual over different regions due to the delayed arrival of the southwest monsoon (June–September), resulting in extended hot and dry spells (Sahana et al. 2015; Rajeev et al. 2022). For instance, the compound hot and dry extremes during post 1980s (in the years 1987, 2009, 2014, and 2015) resulted in a substantial reduction in the staple crop yield across India (Mishra et al. 2020). Similarly, simultaneous or sequential occurrences of heatwaves and heavy precipitation events can pose augmented risks to society in terms of human health, loss of life, and agricultural and infrastructure damage. During recent decades, notable increases in summer heat extremes and monsoonal wet extremes are evidenced over India. For instance, heatwaves in summer and heavy precipitation during the monsoon season

in 1995 and 1998 largely affected many parts of India (Mishra et al. 2022). Similarly, a series of precipitation extremes and heatwaves across India was noted in 2019 (Dhillon 2019; Gupta 2019). Furthermore, warming-induced desiccation is anticipated over most of the urbanized areas in India, indicated through nearly sixfold amplification in compound warm and dry extremes (Ganguli 2023). Despite the increasing risk of compound extremes under the warming climate, considerably less effort has been made to quantify the combined impacts of precipitation and temperature extremes on the societal systems across India (Mukherjee and Mishra 2018; Guntu and Agarwal 2021).

Overall, due to the dense population, rapid urbanization, and agriculture-based economy, the increasing exposure to compound extremes can make India more vulnerable in dealing with the induced impacts. There are three components influencing vulnerability: (i) exposure to extremes, (ii) sensitivity of society to the extremes, and (iii) its capacity to adapt (Wiréhn et al. 2015; Fakhruddin et al. 2019). Vulnerability can be defined as an outcome of these three components that are expected to vary over time and space, thus changing the overall risk from the compound extremes across different regions and time periods. Therefore, it is essential to incorporate the projected spatiotemporal changes in the extreme characteristics to evaluate future risks. In addition, spatiotemporal population dynamics (including population growth and changes in regional population distribution) also plays a vital role in quantifying future vulnerability. To formulate robust mitigation and adaptation planning for India, it is essential to anticipate future risks in terms of prominent climate extremes and associated socioeconomic vulnerability.

To this end, this study focuses on the exposure component of climate change vulnerability. The objective of this study is to estimate the historical and future changes in population exposure to hot-dry and hot-wet compound extremes across the entire Indian mainland. In this regard, the climate observations and future projections from the CMIP6 archive under four future Shared Socioeconomic Pathways (SSPs), i.e., SSP1-2.6, SSP2-4.5, SSP3-7.0, and SSP5-8.5, are considered. The current population estimates and the future period population projections developed based on the SSPs are utilized. Finally, hot spots are identified based on the extent of change in population exposure to the compound extremes and their spatiotemporal evolution under the influence of future warming.

2. Data and method

a. Data

1) Observed climate data

For the period 1951–2020, observed daily gridded maximum temperature data with a spatial resolution of 1° × 1° and precipitation data with a spatial resolution of 0.25° × 0.25° across the entire Indian mainland are accessed from the India Meteorological Department (IMD) (https://www.imdpune.gov.in/lrfindex.php, accessed April 2023). The temperature data with coarse resolution are regridded to a finer resolution of 0.25° × 0.25° via inverse distance weighted (IDW) interpolation to be comparable to the precipitation data.

The observed precipitation data developed by IMD better represent the temporal and spatial variability of the Indian monsoon as compared with the precipitation data from other available sources, e.g., Climate Research Unit (CRU), Global Precipitation Climatology Project (GPCP) version 2.2, and Climate Prediction Center (CPC) Unified rain gauge data, version 1.0 (Mishra et al. 2014; Prakash et al. 2015). To develop the gridded precipitation dataset, daily precipitation information from 6955 rain gauge stations were used. These 6955 stations include 74 agrometeorological observatories, 494 hydrometeorological observatories, and 547 IMD observatories (Pai et al. 2015). The state governments maintain the rest of the rain gauge stations. The density of the stations was spatially nonuniform across the country. However, a reasonable number of stations were considered to well represent the rainfall characteristics over most areas of the country. On average, rainfall records from about 2600 stations per year were available to prepare the daily gridded precipitation data. However, the data density varied from year to year from about 1450 in the beginning year 1901 to about 3950 during the period 1991–94. The inverse distance weighted method was used for interpolating the station measurements into gridded estimates. This method is based on the assumption that the stations closer to the grid location tend to have more similar rainfall characteristics as compared with the distant stations. The weight assigned to each station data decreases as the interpolation point moves farther away from the station. For faster computation, rainfall data from a selected number of nearest neighboring stations (ranging from a minimum of 1 station to a maximum of 4 stations) located within a radial distance of 1.5° around the grid point is considered.

The daily gridded maximum temperature dataset was developed by utilizing daytime maximum temperature recordings collected from 395 stations distributed across India (Srivastava et al. 2009; Rohini et al. 2016). A modified version of Shepard's angular distance weighting algorithm was employed to interpolate the station data into regular grids (Shepard 1968). To mitigate biases in the gridding process, anomaly of daily temperature was used instead of the absolute values. To achieve this, the climatological normal of temperature was estimated for each station based on the period 1971–2000. Before the interpolation, the station data underwent preliminary quality controls, including the removal of outliers and ensuring homogeneity. All stations possessed the same data length to prevent errors in the gridded data arising from inconsistencies in station density. Using the cross-validation technique, RMSE was found to be less than 0.5°C, over most of the country. Relatively larger RMSE was noticed over the hilly areas of Jammu, Kashmir, and Uttarakhand because of lower station density.

2) CMIP6 global climate model simulation data

Future projections of daily maximum temperature and precipitation are retrieved from the repository of NASA Earth Exchange Global Daily Downscaled Projections (NEX-GDDP-CMIP6)

TABLE 1. Global climate models from CMIP6 archive along with corresponding institutions and country of origin.

Serial No.	Model	Modeling group (country)
1	BCC-CSM2-MR	Beijing Climate Center (China)
2	EC-Earth3	EC-Earth-Consortium (Europe)
3	GFDL-ESM4	NOAA/GFDL (United States)
4	INM-CM4-8	Institute for Numerical Mathematics (Russia)
5	MPI-ESM1-2-HR	Max-Planck-Institute for Meteorology (Germany)
6	MRI-ESM2-0	Meteorological Research Institute (Japan)
7	NorESM2-MM	NorESM Climate modeling Consortium (Norway)

(Thrasher et al. 2022). The archive is composed of downscaled values with a spatial resolution of 0.25° × 0.25° for the historical and future time period, developed utilizing the outputs obtained from multiple general circulation models (GCMs), taking part in phase 6 of the Coupled Model Intercomparison Project (CMIP6). Downscaling was carried out using the bias-correction spatial disaggregation (BCSD) method, which is a statistical downscaling algorithm. Past studies reveal that the NEX-GDDP-CMIP6 outputs are found to well depict the long-term precipitation and temperature conditions and corresponding changes over time considering different regions across the globe (Park et al. 2022; Murali et al. 2023; Wang et al. 2023; Zhang et al. 2023). As it is generally agreed that projections of future climate change should not rely on a single model (Jebeile and Crucifix 2020), a total of seven GCMs are chosen and corresponding downscaled data for the aforementioned variables are used. These seven models are selected based on their potential to capture the spatiotemporal variability in precipitation and temperature (with reference to the observed data) across the Indian mainland, as revealed by past studies (Katzenberger et al. 2021; Mitra 2021; Jose et al. 2022; Thakur and Manekar 2022). Furthermore, model simulations from seven GCMs seem to be adequate to draw inferences regarding future changes in the precipitation- and temperature-based climate regimes across India (Tegegne et al. 2019; Wang et al. 2020). A few basic details regarding the chosen models are provided in Table 1, including their modeling groups and countries. Simulated data of precipitation and maximum temperature are obtained for four SSPs based on different categories of future socioeconomic developments. The considered SSPs are as follows: the first one is SSP1-2.6, which represents the sustainability socioeconomic scenario incorporating lower radiative forcing of 2.6 W m^{-2}; the second one is SSP2-4.5, indicated as the middle of the road scenario with a moderate radiative forcing of 4.5 W m^{-2}; the third one is SSP3-7.0, which corresponds to the regional rivalry socioeconomic pathway with medium to high radiative forcing level of 7.0 W m^{-2}; and the fourth one is SSP5-8.5 that portrays the fossil-fuel-driven future development scenario with higher end of the forcing pathway with 8.5 W m^{-2} radiative forcing (Cook et al. 2020). The first realization (r1i1p1) corresponding to each model is considered.

3) HISTORICAL POPULATION DATA

Historical population data for the entire Indian mainland are collected from the NASA Socioeconomic Data and Applications Center (SEDAC) (CIESIN 2018a). This GPWv4 (Gridded Population of the World, 4th version) dataset consists of grid-wise human population counts created by extrapolating the raw census estimates from the national population registers for a series of target years: 2000, 2005, 2010, 2015, and 2020. To develop these data, population statistics from nearly 13.5 millions of administrative divisions of national and subnational domains across the globe are utilized, and a uniform areal weighting technique was employed to assign population counts to the 30 arc-s (0.008 333°) grids (CIESIN 2018b). The primary advantage of disaggregating the demographic variables like population by areal weighting is to maintain fidelity to the raw input data. For India, the input population statistics are considered at administrative level 3 (Doxsey-Whitfield et al. 2015), which is the highest spatial disaggregation of population data. Further, GPWv4 allocates the population within each administrative division to keep the population consistent, corresponding to the grids lying within the said division (Chen et al. 2020). These datasets are accessible at a native resolution of 30 arc-s (0.008 333°), as well as four coarser resolutions: 2.5 arc-min (0.041 667°), 15 arc-min (0.25°), 30 arc-min (0.5°), and 1°. We extracted the data at a 2.5 arc-min (approximately 5 km) spatial resolution and regridded to 0.25° × 0.25° resolution, to make it compatible with other climate data. Regridding of the data is done through upscaling, i.e., summing up the population values of all the smaller grids (2.5 arc-min) falling within a target grid (0.25° × 0.25°) (Iyakaremye et al. 2021).

4) FUTURE POPULATION PROJECTIONS

The future population projection datasets are also extracted from the NASA SEDAC. These future datasets are available at a spatial resolution of 0.125° × 0.125° for different SSPs, at 10-yr intervals for the time period 2010–2100 (Jones and O'Neill 2016; Sun et al. 2021). As mentioned before, these SSPs illustrate four distinct potential future states of the society based on the trends in technological progress, demography, economy, governance, lifestyle, and other societal aspects. The population projections based on the SSPs were downscaled by utilizing a gravity-type spatial allocation model calibrated with historical data (Jones 2014). The gravity-type model is based on population potential (Stewart 1942) and produces scenario-dependent projections. Population potential can be interpreted as a measure of the influence that the population at one location exerts on another location, e.g., high potential is obtained at locations existing in closer

proximity to densely populated areas. The population projections are qualitatively congruent with the underlying assumptions made regarding spatial development patterns in the SSPs, and quantitatively consistent with the future estimates of national population and urbanization. In this study, simulated data for four different SSPs are considered. These are SSP1-2.6, SSP2-4.5, SSP3-7.0, and SSP5-8.5. The projected future population datasets are regridded to 0.25° × 0.25° spatial resolution for spatial resolution uniformity with other data.

b. Method

1) Joint hot-dry and hot-wet extreme indices

The methodological flowchart is presented in Fig. 1 that starts with the development of the Joint Extreme Index (JEI). Statistical approach to develop the JEI is utilized from a recent work by the authors (Dash and Maity 2021). A summarized version is as follows. We pick out three extreme indices: warm-spell duration index (WSDI) reflects extreme hot weather spells, consecutive dry days (CDD) reflects consecutive low precipitation events that may lead to extreme dry spells, and extreme wet days (EWD) index that reflects heavy precipitation events. Out of the three indices, WSDI and CDD are developed by the Climate Variability and Predictability (CLIVAR) project of the World Climate Research Programme jointly with the Expert Team on Climate Change Detection and Indices (ETCCDI) (https://www.wcrp-climate.org/data-etccdi, accessed in April 2023). EWD was newly incorporated and is based on a percentile-based local threshold to capture the substantial spatiotemporal variability in the precipitation climatology in a vast country like India (Dash and Maity 2021). Details of these indices are provided in Table 2. The extreme indices and their corresponding percentile thresholds are computed utilizing the daily precipitation and temperature data for the entire year. The primary focus of this study is to identify the changes in compound precipitation–temperature extremes on an annual basis. Thus, the inherent seasonality is not separated while computing the thresholds. The compound extremes are defined as the occurrence of two simultaneous or successive extremes within a 10-day time interval, as elaborated further. Considering a specific year, first, the hot extremes (WSDI) are identified, which is defined as six or more consecutive days (denoted as m days in Fig. 1) exhibiting daily maximum temperature >95th percentile. The wet extreme (EWD) corresponds to simultaneous and/or successive occurrence of heavy precipitation events within n days (here, $n = 10$) preceding and succeeding the hot extreme. Similarly, the dry extremes (CDD) refer to the dry conditions persisting within the entire preceding and succeeding n days centered around the hot extreme duration.

Joint distributions between WSDI and CDD (hot-dry extreme events) and WSDI and EWD (hot-wet extreme events) are developed using copulas considering each of the constituting index as a random variable (say X and Y). In probability theory, a copula is a function that combines the one-dimensional marginal distribution functions of two or more random variables to produce a joint distribution function of those variables (Maity 2022). Sklar's theorem states that joint probability distribution can be represented via a copula function and the corresponding univariate marginal distribution functions (Serinaldi et al. 2009). For example, given two random variables, X and Y with cumulative distribution functions $F_X(x) = P(X \le x)$ and $F_Y(y) = P(Y \le y)$, the joint cumulative distribution of X and Y is as follows:

$$F_{X,Y}(x, y) = P(X \le x,\ \ Y \le y) = C[F_X(x),\ \ F_Y(y);\ \ \theta], \quad (1)$$

where C is the copula function of the marginal distribution functions, $u = F_X(x)$ and $v = F_Y(y)$ for the random variables X and Y, such that for all x, y in $\overline{R} \in (-\infty, \infty)$; θ is the parameter of the copula function.

Using the kernel density estimator, nonparametric estimates of the marginal probability distributions are computed (Maity and Kumar 2008). The association between the two random variables is estimated in terms of Kendall's tau τ, which is a scale-free measure of association.

We initially selected three Archimedean copulas, that is, Clayton, Gumbel–Hougaard, and Frank, and the best-fit one was chosen for deriving the joint distribution. Table 3 represents a few mathematical descriptions of the copulas. The best-fit copula is chosen via goodness-of-fit test utilizing two statistics, i.e., Kolmogorov–Smirnov T_n and Cramér–von Mises S_n (Maity 2022). A better fit is indicated through lower values of these statistics. After getting the best-fit copula, the joint distribution is obtained by employing Eq. (1).

The JEI is derived following standardization of the joint probability estimates through the inverse standard normal distribution. The JEI is therefore, mathematically represented as

$$\text{JEI} = \Phi^{-1}[F_{X,Y}(x, y)], \quad (2)$$

where Φ^{-1} is the inverse standard normal distribution function.

2) Computation of trends

To identify the trends in the joint extreme indices, the Mann–Kendall (MK) trend test is used at a statistical significance level of 0.05. The MK test is a nonparametric approach that takes into account the rank of the data rather than the actual values, making the computation less sensitive to the distribution of data. In addition, it is less affected by inhomogeneity, abrupt breaks, and nonlinear trends in the time series (Tabari et al. 2011).

3) Population exposure

Population exposure E to the compound extremes is computed by multiplying the number of years with above-normal values joint extreme index (i.e., JEI > 0) with the corresponding mean population count P at each grid location over a specified time period. It is expressed in person-years:

$$E = N_{\text{JEI}} \times P, \quad (3)$$

where N_{JEI} indicates the number of years with above-normal joint extreme and P is the population.

Change in the population exposure to compound extremes at a particular grid location can result from changes in the

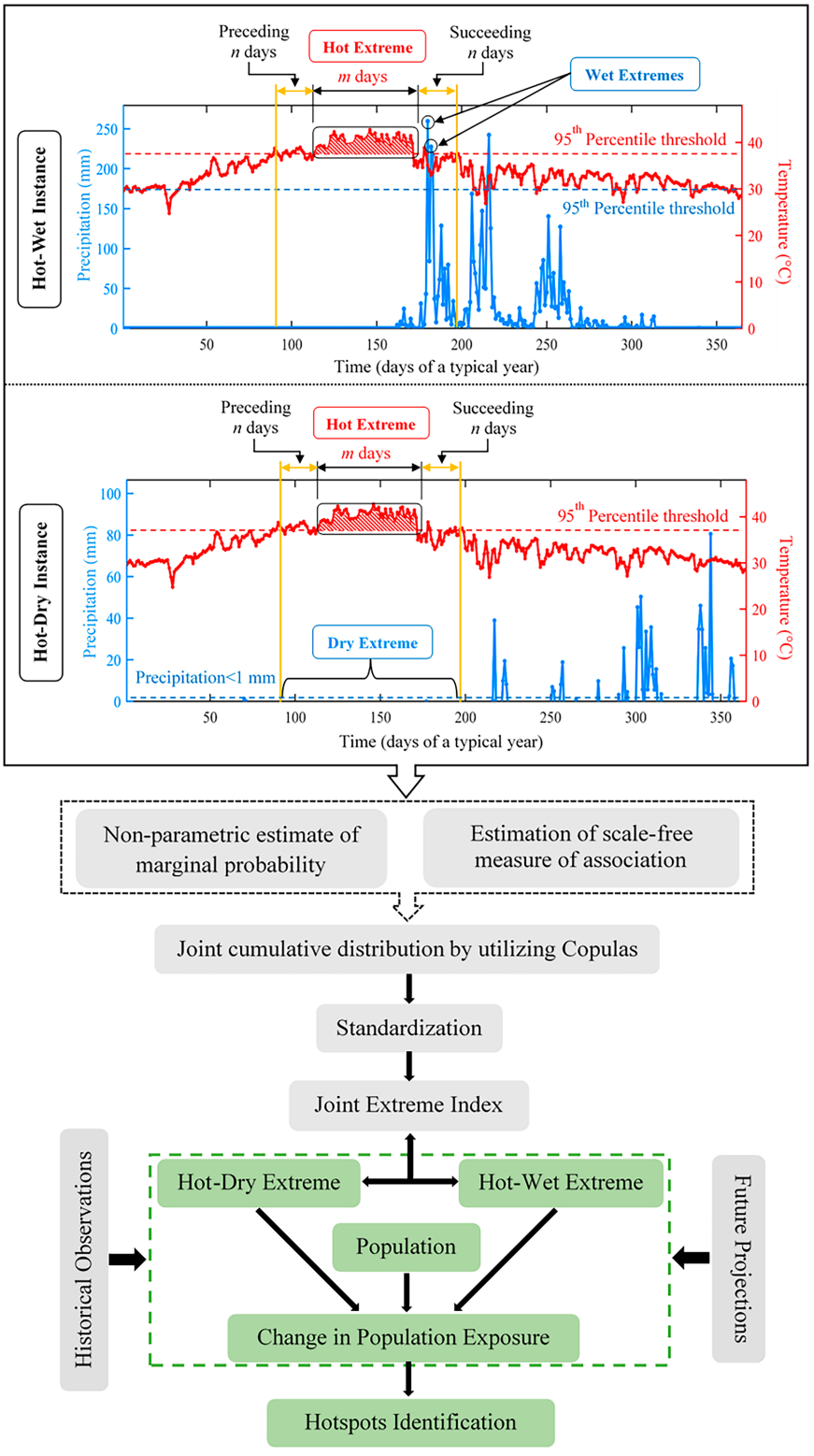

FIG. 1. Methodological outline showing joint index of compound extremes and population exposure.

TABLE 2. Details of precipitation and temperature extreme indices. Here, ID indicates identifier.

Index ID	Index name	Description
EWD	Extreme wet days	Days with precipitation > 95th percentile of the daily precipitation amount during the base period, 1981–2010
CDD	Consecutive dry days	Max no. of consecutive days with precipitation of <1 mm
WSDI	Warm-spell duration index	No. of days in a year with at least 6 consecutive days when daily max temperature (TX) > 95th percentile (corresponding to the TX during the base period 1981–2010)

population count or change in the compound extreme occurrences or changes in both population and compound extreme conditions. Hence, the change in population exposure is estimated by considering three contributing factors, i.e., (i) population change, (ii) climate change, and (iii) combined change, across two comparable time periods. The climate influence is estimated by multiplying the change in N_{JEI} with the baseline population. In other words, the impact of climate change on the exposure is separated by keeping the population constant at the reference time period and allowing the climate to evolve according to the future projections. Similarly, the population influence is obtained by multiplying the population change across the two time periods with the N_{JEI} in the reference time period. The combined influence integrates concurrent change in both the factors. The total change in population exposure to compound (ΔE) can be expressed as

$$\Delta E = (\Delta N_{\mathrm{JEI}} \times P_{\mathrm{ref}}) + (N_{\mathrm{JEI;\,ref}} \times \Delta P) + (\Delta N_{\mathrm{JEI}} \times \Delta P), \tag{4}$$

where $(\Delta N_{\mathrm{JEI}} \times P_{\mathrm{ref}})$, $(N_{\mathrm{JEI;ref}} \times \Delta P)$, and $(\Delta N_{\mathrm{JEI}} \times \Delta P)$ are the climate influence, population influence, and the combined influence on the change in exposure, respectively; P_{ref} is the population in the reference period; ΔP is the change in the population; $N_{\mathrm{JEI;ref}}$ is the number of years with above-normal JEI values in the reference period; and ΔN_{JEI} is change in the number of years with above normal JEI w.r.t. the reference period.

4) IDENTIFICATION OF HOTSPOTS

Hotspots are identified based on the extent of future changes in population exposure to the joint compound extremes, i.e., hot-wet and hot-dry events. Toward this, a hotspot metric is utilized, denoted as $\mathrm{HSP}_{\Delta E}$—the greater the change in the exposure levels between two considered time periods is, the greater the sensitivity will be. For a particular grid location, $\mathrm{HSP}_{\Delta E}$ is computed based on the change in population exposure in that grid between the historical and future time periods with respect to the 95th-percentile threshold change considering all the grids over India:

$$\mathrm{HSP}_{\Delta E} = \sqrt{\frac{(\Delta E)^2}{[P_{95}(|\Delta E|)_{\text{all grids}}]^2}}, \tag{5}$$

where ΔE denotes the change in population exposure between historical and future time periods; $P_{95}(|\Delta E|)_{\text{all grids}}$ represents the 95th percentile threshold value of the absolute difference in exposure change considering all the grid locations.

TABLE 3. Details of three considered Archimedean copulas. In the third column, \{0} indicates that 0 is excluded from the indicated continuous range.

Copula	Copula function, $C(u, v)$	Copula parameter $\theta \in$
Frank	$\frac{-1}{\theta}\ln\left[1 + \frac{(e^{-\theta u}-1)(e^{-\theta v}-1)}{(e^{-\theta}-1)}\right]$	$(-\infty, \infty)\backslash\{0\}$
Clayton	$[\max(u^{-\theta} + v^{-\theta} - 1{,}0)]^{-1/\theta}$	$[-1, \infty)\backslash\{0\}$
Gumbel	$\exp\{-[(-\ln u)^{\theta} + (-\ln v)^{\theta}]^{1/\theta}\}$	$[1, \infty)$

3. Results and discussion

a. *Spatiotemporal changes in the extreme hot, dry, and wet events*

First, the spatiotemporal changes in the individual hot, dry, and wet extremes are evaluated across India. The annual hot, dry, and wet extreme characteristics are expressed through three extreme indices, WSDI, CDD, and EWD, respectively. The entire historical time period (1951–2020) is divided into three epochs, i.e., pre-1980 (1951–80, T1), post-1980 (1981–2000, T2), and the recent two decades (2001–20, T3). As a climate regime shift occurred around 1980s across India (Sahana et al. 2015; Cho et al. 2016; Pattanayak et al. 2017; Ross et al. 2018; Shrestha et al. 2019; Dash and Maity 2019), 1980 is considered as the partitioning year here. Centering around 1980, two epochs, i.e., T1 and T2 are constructed. Further, the most recent two decades, T3, is considered separately to identify the relative extent of changes in the most recent times relative to the immediate pre- and post-1980s. Figures 2 and 3 show the mean and standard deviation of the extreme indices, respectively, during the pre-1980s period (T1) and the consequent changes (expressed in percentage) during the recent time epochs, i.e., T2 and T3. As the hot, dry, and wet extremes portray the extreme frequency/duration characteristics, the mean of the extreme conditions represents the annual average number of days with respective extreme conditions during the concerned time period. Similarly, through the standard deviation, the extent of dispersion or variability of the respective extreme around the mean state is expressed. Furthermore, the percentage difference in the mean and standard deviation of the extremes during T2 and T3 are computed with respect to that during T1. Percentage increase (decrease) in the mean of extreme indices indicates increase (decrease) in the frequency of extreme wet and the duration of dry or hot conditions in the subsequent period. Similarly, percentage

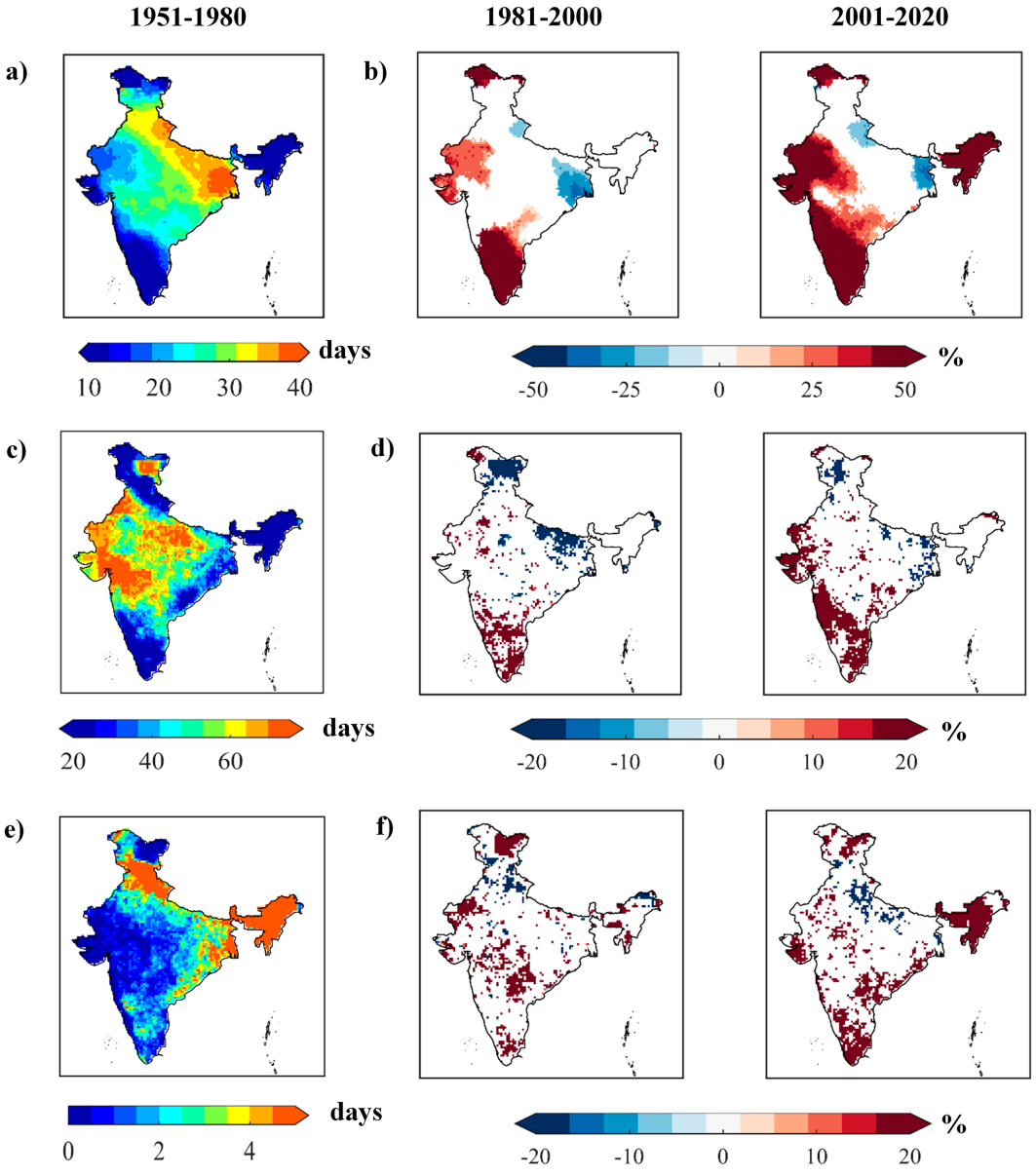

FIG. 2. Spatial variation of (a) average duration of hot spells (WSDI) during 1951–80 (T1), and (b) its change in percentage during 1981–2000 (T2) and 2001–20 (T3). (c),(d) As in (a),(b), but corresponding to dry spells (CDD). (e),(f) As in (a),(b), but corresponding to extreme wet days (EWD). White patches in (b), (d), and (f) indicate insignificant changes at 5% significance level.

increase or decrease in standard deviation indicates the increase or decrease in the interannual variations/fluctuations in the extreme hot or wet or dry conditions. Statistical significance of the percentage changes in mean and standard deviation are evaluated using the *t* test and F test (Maity 2022), respectively, at 5% significance level. Considering the extreme hot spells, higher mean (>30 days) and variability (>15 days) are noticed over northern and eastern regions during the pre-1980s (T1). In contrast, a more prominent change in hot spell (>50%) is witnessed across the southern and northwestern regions in the next two epochs (T2 and T3). Additionally, spatially more extensive and intense changes are noticed during T3. Longer dry spells are noticed across the western and northern regions during T1. In T2 and T3, the dry extreme has increased (decreased) across southern regions and western coastal regions (eastern regions). Higher variability in the dry spell is noticed across the north Himalayan, western, and Indo-Gangetic regions in T1, whereas lower variability is noted over the northeast and southernmost regions. However, in the subsequent epochs, dry extremes have become more variable across the southern regions. Considering the wet extremes, higher mean is noticed across northeast,

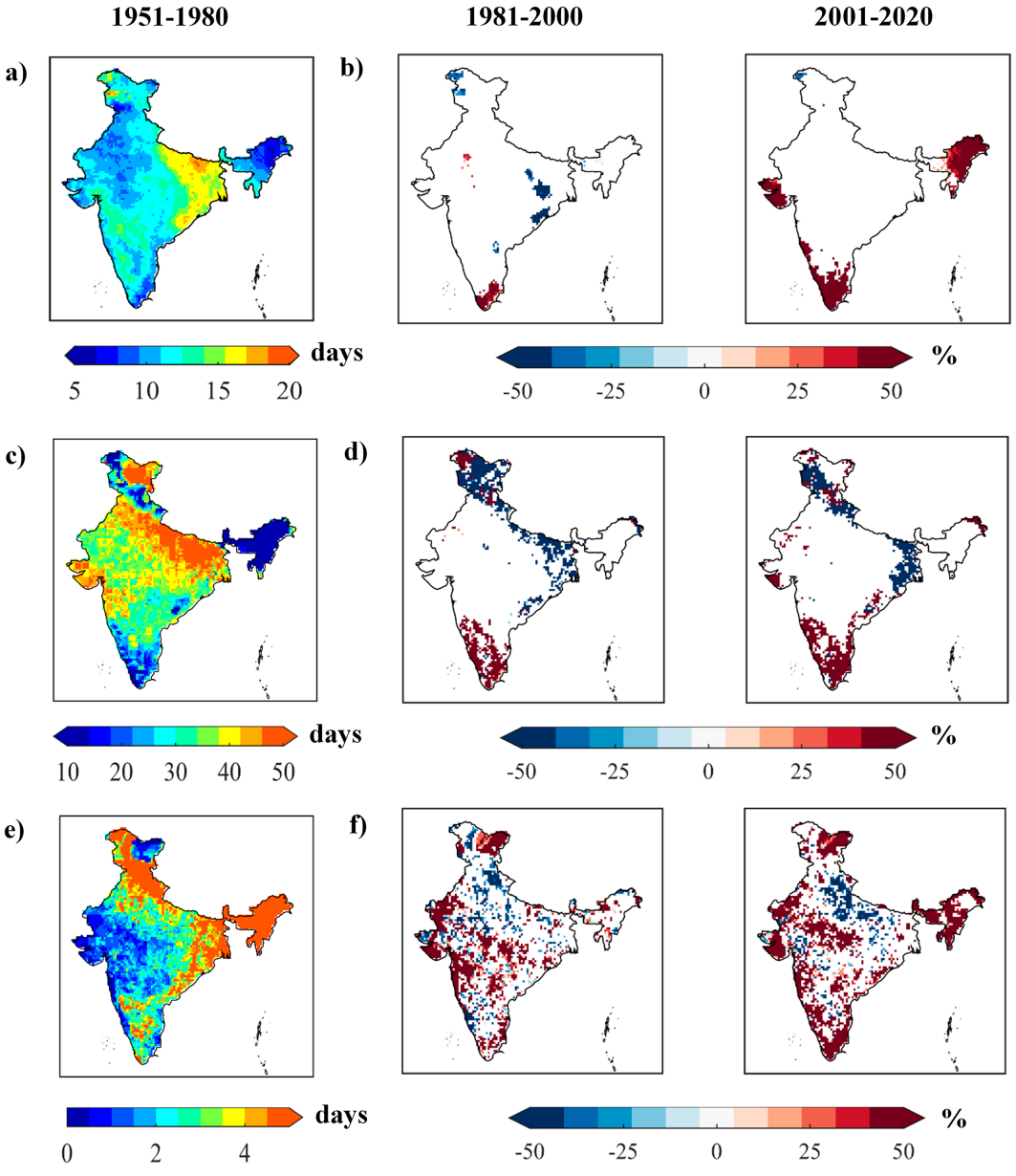

FIG. 3. As in Fig. 2, but for standard deviation.

eastern coastal, and a few patches over the northern regions during T1. Increased variability of wet extremes is noticed across the southern regions of India. During T3, extensive increase in mean as well as variability of wet extremes is noted as compared with T2. However, the increasing variability in wet extremes is found to be more intense and spatially extensive as compared with the increase in mean. Over the northeast regions of India, the wet extremes exhibited increases in both mean and variability during the most recent times (T3). Apart from that, the coastal regions have experienced more frequent wet extremes during T3.

Overall, precipitation and temperature extremes expressing hot, dry, and wet conditions have increased in the recent time periods, i.e., T2 and T3 with reference to T1, in many parts of India, whereas the same has decreased in some regions, all with respect to the local climatology. However, the most prominent increase in the spatial extent with increasing extreme conditions is found during T3.

b. Compound hot-dry and hot-wet extremes

Compound extreme refers to the combination of multiple extremes contributing to larger societal and environmental risks (Zscheischler et al. 2018). To characterize the compound hot-dry and hot-wet extremes, two joint extreme indices (JEIs) are developed using the joint probability distribution between temperature (hot) and precipitation (wet/dry) based

extreme indices constructed through copulas (Salvadori and De Michele 2004). For deriving the JEIs, 1951–80 is considered as the base period. Properties of the JEI in relation to its constituting precipitation and temperature extreme indices are illustrated through their respective time series in Fig. S2 in the online supplemental material for the entire time period, 1951–2020. The JEI for hot-wet extreme is presented along with individual hot (WSDI) and wet (EWD) extreme indices for one grid location. High (low) magnitude of JEI is noticed when the constituting indices magnitudes are high (low). For instance, the above-normal hot-wet extreme (JEI > 0) in the year 2016 is obtained for the individual hot and wet extremes with above-normal magnitudes. This portrays the underlying characteristics of the JEI in combining both extreme temperature and precipitation conditions. However, the JEI magnitude may or may not be high when either of the constituting indices is high, based on the combined status of temperature and precipitation extremes. One such instance of this can be noted for the year 1989, where the wet extreme of higher magnitude and below-normal hot extreme resulted in the above-normal magnitude of hot-wet extreme conditions. This attribute of the JEI infers that the combined status may result in amplified consequences, although the constituting variables are not at their extreme extents.

Further, the spatial distribution pattern of the hot-dry and hot-wet compound extremes alongside the constituent hot, wet, and dry extremes are presented to evaluate the feasibility of the developed JEI in capturing the combined extreme conditions across different regions. In this regard, two years, i.e., 2009 and 2019 (Fig. S3 in the online supplemental material) are selected, as during these years, many regions of India experienced the hot-dry (in 2009) and hot-wet (in 2019) extreme conditions, as reported by past literatures (Mishra et al. 2020; Nayak et al. 2022). The compound extreme magnitude is found to be severe over the regions possessing high precipitation and temperature extreme occurrences during both the years. For instance, in 2009, above-normal hot extreme spells are noted over most of the country, wherein relatively higher values were confined across the northern, western coastal, and some eastern regions. Similarly, the northwest, Indo-Gangetic Plain, and southern coastal parts exhibited higher dry extremes. Considering both hot and dry conditions together, the western coastal regions and scattered areas over northern and eastern regions are noticed with above-normal hot-dry extreme occurrences. A similar observation is noted considering the hot-wet compound extreme, wherein mainly the northeast, western, and eastern coastal regions are noticed with the above-normal conditions. The above discussion suggests that the JEI captures the compound extremes well across space and time and can be useful in evaluating the hot-wet and hot-dry compound extreme characteristics.

Next, the spatiotemporal changes in compound hot-dry and hot-wet extremes are evaluated for entire India in terms of its magnitude and frequency during the period 1951–2020. Frequency of the compound extremes are presented in Figs. 4a and 4b as the percentage years with above-normal occurrences of hot-dry and hot-wet extremes, respectively, during T1 (1951–80), T2 (1981–2000), and T3 (2001–20). For both the extremes, frequency has gradually increased over time with the least percentage of years and spatial coverage during T1 to the maximum extent of occurrence with notably wider spatial spread during T3. The frequency of hot-wet extreme has increased more intensely across northeast, eastern coastal and southern regions. More frequent and spatially extensive hot-dry extremes are experienced over the southern and western parts of the country. Consequently, the southern regions of the country have experienced a simultaneous increase in hot-dry and hot-wet compound extreme occurrences over time as compared with the other parts of the country.

Significant trends in the magnitude of compound hot-wet and hot-dry extremes are assessed by the Mann–Kendall trend test (5% significance level) for two time epochs: 1951–80 and 1981–2020. Trends in compound extremes refer to gradual and continuous change within a particular period. Figure S4 in the online supplemental material shows the spatial pattern of significantly decreasing and increasing trends in hot-dry and hot-wet extremes across India. Like the frequency of the compound extremes, the significant increase in the magnitude has become spatially extensive during the recent epoch (1981–2020) as compared with the later epoch, 1951–80. Significant increases in the hot-dry extremes are noticed across the eastern and western regions of India. The hot-wet extremes are becoming more intense, mainly across the western and northeast regions of the country, along with the eastern coastal regions. Further, a more extensive spatial spread with increasing compound extremes is noticed for the hot-wet extreme as compared with the hot-dry extreme. Moreover, similar to the individual hot, wet, and dry extremes, the compound hot-dry and hot-wet extremes have increased to the maximum extent with respect to frequency and magnitude during the recent most times than ever before. In addition, out of the two compound extremes, hot-wet extremes have become more frequent and intense, along with increased spatial coverage across the country.

c. *Historical changes in population exposure to the compound extremes*

Next, changes in exposure from the compound extremes on the human population are assessed across India during the historical period, 1981–2020. Before moving to the population exposure context, a brief idea regarding the population distribution in India and the compound extremes across regions with similar population density is discussed. The spatial pattern of population distribution during the years 2000 and 2020 is shown in Figs. 5a and 5b, along with the percentage changes in population across the two decades (Fig. 5c). A higher population density of about >3 lakhs (1 lakh = 100 000) per ($0.25° \times 0.25°$) size grid is noted over the entire Indo-Gangetic Plain, the southernmost regions, and the eastern and western coastal parts. The less populated regions are noted in the north Himalayan, northeast, northwest, and some eastern regions; these include the hilly, desert, and dense forest regions of the country. From 2000 to 2020, the population has expanded across many regions of the country, more extensively across the northern regions mainly. Most of the country has evidenced about 20% or more

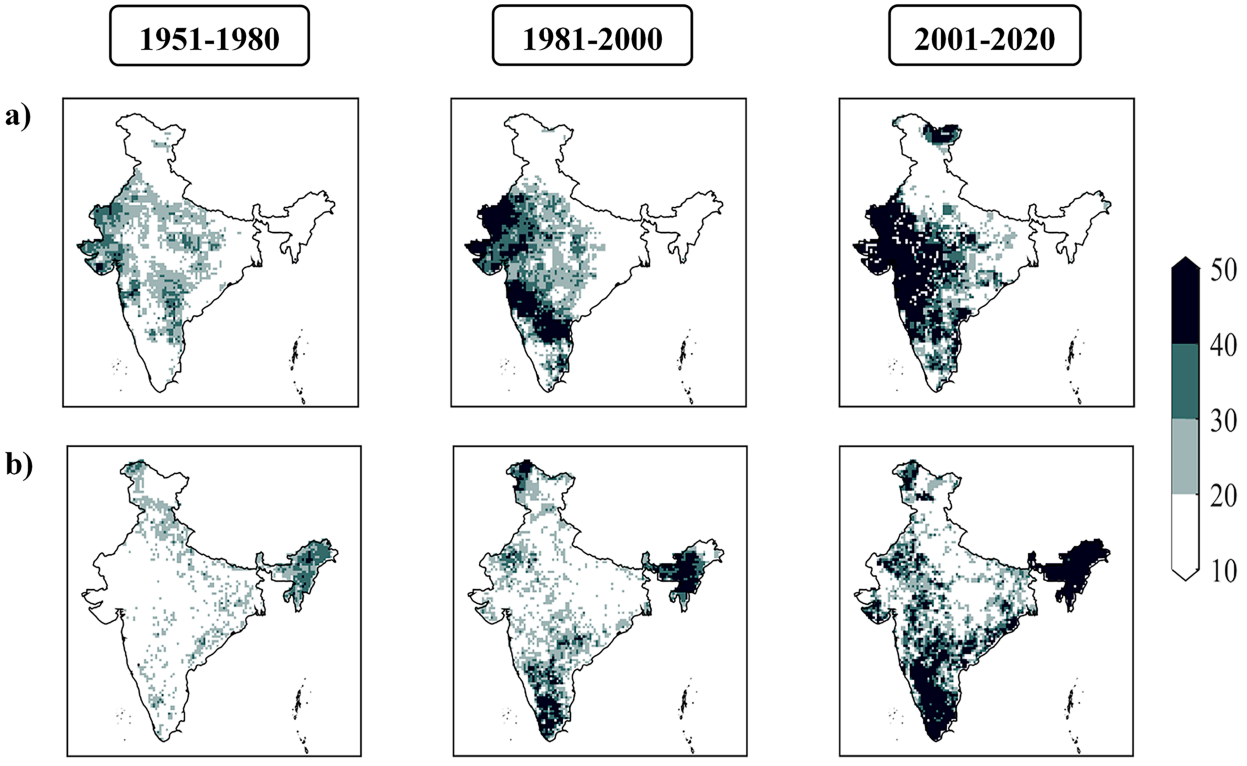

FIG. 4. Occurrences (percentage of years) of above-normal compound extreme events (base period: 1951–80) across India. Spatial variations are presented for (a) hot-dry extreme and (b) hot-wet extreme during three time periods: (left) 1951–80 (T1), (center) 1981–2000 (T2), and (right) 2001–20 (T3).

increase in the population, with very few scattered patches of population shrinkage. Furthermore, the maximum extent, i.e., >50% of change is concentrated across Bihar, Jharkhand, Meghalaya, and Rajasthan, with a few patches across some of the remaining states.

Based on the grid-wise current (in 2020) population strength, the country is classified into four categories populated regions (Fig. S5a in the online supplemental material), that is, low (population < 1 lakhs), moderate (1–2 lakhs), high (2–3 lakhs), and very high (>3 lakhs). Figures S5b and S5c illustrate the percentage of the area (spatial extent) with significantly increasing/decreasing changes considering each of the four populated regions during 1981–2020. A spatially more extensive increase in hot-wet extreme is noticed over the low-populated regions. Further, for the other three categories of populated regions (moderate, high and very high), comparatively less area with changes is found. For the hot-dry extreme, a more or less similar spatial extent with significant changes is noticed across the four regions. However, relatively higher areal extent with increasing hot-dry extreme is observed for the low and moderately populated regions. Considering the regions with higher population density, significant increase in the hot-wet extremes is found to be spatially more extensive as compared with the hot-dry extremes.

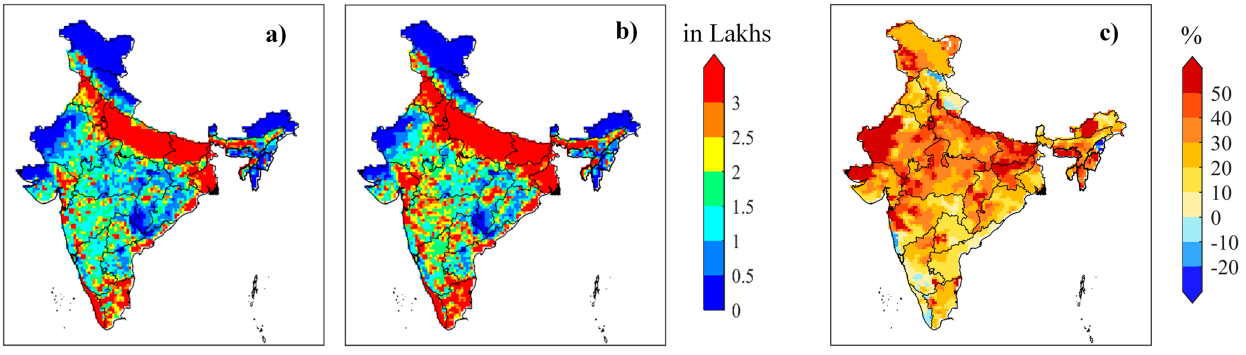

FIG. 5. Spatial distribution of population in (a) 2000 and (b) 2020 across India, along with the (c) percentage change between 2000 and 2020.

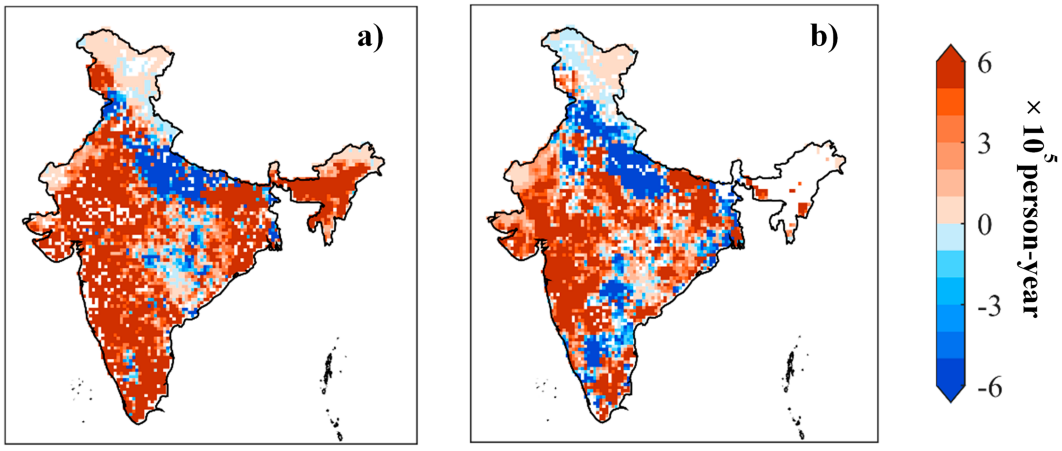

FIG. 6. Historical changes in population exposure to the compound (a) hot-wet and (b) hot-dry extremes expressed in person-years during 1981–2020, across India.

Figure 6 shows the spatial pattern of historical changes in population exposure (in person-year) across India during 1981–2020. Toward this, the entire time period is divided into two epochs of 20 years each, i.e., 1981–2000 and 2001–20. The changes in population exposure between the two epochs are estimated (as presented in section 2b) for the hot-dry (Fig. 6a) and hot-wet (Fig. 6b) extremes. Increased exposure from the two compound extremes is noticed across most of the country, with a few regions noticed with decreased exposure. Southern, western, and eastern parts of the country exhibited a higher increase in population exposure from hot-wet extremes, whereas the northern and central parts experienced reduced population exposure. On the other side, higher growth in population exposure from hot-dry extremes is noticed across the western, eastern coastal, and southernmost regions mainly. Furthermore, across the coastal regions, increased exposure is evidenced for both extremes. The hilly regions, along with the western most regions adjacent to Rajasthan and Gujrat are found with the least change in population exposure to the compound extremes. Spatial extent with maximum increase (>5 lakhs person-year) in the exposure is found to be more prominent in the case of hot-wet extreme as compared with the hot-dry extreme.

d. *Future changes in population exposure to the compound extremes*

Next, changes in the population exposure to the hot-dry and hot-wet events are assessed for the future period, 2021–2100 with reference to the historical period, 1981–2020. Toward this, the entire future period (2021–2100) is divided into near-future (2021–60, F1) and far-future (2061–2100, F2) periods. The change in population exposure for the near-future and far-future periods is evaluated considering the projected climate and population estimates for four SSPs, i.e., SSP1-2.6, SSP2-4.5, SSP3-7.0, and SSP5-8.5 (hereinafter SSP1, SSP2, SSP3, and SSP5, respectively).

Prior to estimating the future exposure, the resemblance between the historical observations and future estimates in capturing the compound hot-wet and hot-dry extreme characteristics is evaluated. The compound extremes derived from future projections are compared with that of the observations for the 7-yr intersecting duration, 2015–21 (as the future projection is available from 2015). Based on the outcomes, different sets of combinations (Table S1 in the online supplemental material) of the seven GCMs are selected with respect to hot-dry and hot-wet extremes for further analysis. Figures S6 and S7 in the online supplemental material display frequency (in percentage of years) of hot-dry and hot-wet extremes, respectively, for historical and future projections under the four SSPs. There are some minor deviations between the observed and future projected compound extreme conditions. These are expected primarily due to the assumption-based future warming and socioeconomic development scenarios (reflected through the four SSPs). Second, in general, the discrepancies in observed and modeled extreme conditions can be attributed to the uncertainties in various aspects, including model uncertainty (assumptions in different GCMs), bias correction approach, downscaling method, and method for deriving the compound extremes (Jha et al. 2023; Meng et al. 2022). Still, a notable resemblance between the observations and model projections is obtained for both hot-dry and hot-wet extremes considering all four SSPs. Furthermore, a relatively higher resemblance is captured in the case of hot-dry extremes as compared with that of the hot-wet extremes. Out of all the four SSPs, the projected conditions under SSP3 have relatively more resemblance with the observed spatial pattern for the hot-wet extremes. On the other hand, for the hot-dry extreme, a more/less similar degree of agreement is noted between the observed and future projected conditions under all four SSPs. Regions experiencing more frequent occurrences of compound extremes are captured well for both hot-wet and hot-dry conditions, whereas regions experiencing less frequent compound extremes are noticed with deviations in the model projections. For both the extremes, overestimation is noticed across the western Rajasthan regions. However, across the northeast regions, frequency of the hot-wet extremes

is underestimated. Considering the spatial extent exhibiting above-normal compound extremes, an overestimation in the case of hot-wet extremes and an underestimation in hot-dry extremes is noticed during 2015–21. Overall, some regions are noted with highly resembling spatial patterns of observed and projected compound extremes and some regions are noted with small deviations from the observed conditions.

Figures 7 and 8 represent changes in population exposure to the hot-dry and hot-wet extremes, respectively, during the near- and far-future (F1 and F2) periods under the four SSPs. A significant increase in future exposure is noticed as compared with the baseline period 1981–2020. More than 10 million person-year increase in exposure is noticed across many regions of the country considering both extremes. However, the maximum extent of spatial coverage with higher exposure is found in the case of SSP3 and the least in the case of SSP1. The exposure from hot-wet extreme is expected to increase more extensively as compared with the hot-dry extreme under all the SSPs. Further, relatively higher exposure change is captured across the country during the far future period as compared with that obtained during the near future period. The exception is noted under SSP5 and SSP1 for the hot-dry conditions, wherein reduced spatial extent with higher exposure increase is noticed during F2 as compared with F1. Over the entire Indo-Gangetic region, an increase in the future population exposure is expected to be more than 10 million person-year during F2, considering both hot-wet and hot-dry extremes, consistently across all the four SSPs. Apart from this, prominent increases in the population exposure from hot-wet (hot-dry) extremes are mostly confined across the southern and northeast (southern and western) regions. The southernmost parts of India are expected to experience a more pronounced increase in the population exposure from the hot-wet extremes. However, the contrast is noticed considering the hot-dry conditions. Over the central parts of India, the exposure is going to be more from the hot-dry extremes as compared with the hot-wet extremes.

Next, hotspots are identified based on the extent of changes in future exposure from the hot-dry and hot-wet extremes for the four SSPs. Considering the exposure change ΔE in all grid locations over the country, the 95th percentile value is identified. Following this, a hotspot metric, $\mathrm{HSP}_{\Delta E}$ (as discussed in section 2b), is calculated for each grid relative to the threshold (i.e., relative to the grid exhibiting the 95th percentile threshold). It can be noted that the grids possessing an exposure increase greater than the threshold value have $\mathrm{HSP}_{\Delta E} > 1$. Furthermore, four regions are defined with different relative extents of increasing exposure based on the hotspot metric, i.e., low ($\mathrm{HSP}_{\Delta E} \leq 0.2$), moderate ($0.2 < \mathrm{HSP}_{\Delta E} \leq 0.6$), high ($0.6 < \mathrm{HSP}_{\Delta E} \leq 1$), and very high ($\mathrm{HSP}_{\Delta E} > 1$) population exposure to compound extremes. Figure 9, along with Fig. S8 in the online supplemental material, show the spatial pattern of the four regions for hot-dry and hot-wet extremes, respectively, during F1 and F2. The spatial pattern of very high exposure regions for the respective compound extreme is noticed to be more or less similar under the four SSPs. Comparatively, more areal extent with very high and low exposure level is noted for the hot-wet extremes than that of the hot-dry extremes. On the other hand, the moderate and high exposure regions are spatially more extensive for hot-wet extremes. Further, the hilly regions across the north Himalayan and northeast regions and parts of Gujarat, Rajasthan, and Odisha are expected to be the least affected from increasing population exposure to compound extremes across all the SSPs and time periods. Considering the two future periods, areal extent with high and very high exposure to hot-wet and hot-dry extremes tends to increase over time, that is, from F1 to F2 across the Indo-Gangetic regions. On the contrary, the same is noted to be decreasing with time across the southwestern regions. Furthermore, areas in the Indo-Gangetic Plain are found to be the future hotspots (very high population exposure) to both hot-dry and hot-wet extremes, considering all the projected warming and population conditions. It can be noted that these are the densely populated regions in the country based on current population strength (Fig. S5a in the online supplemental material). Apart from this, scattered locations across the southernmost regions (entire Kerala, southern Karnataka, and parts of Tamil Nadu) are noticed with very high population exposure to the hot-wet extremes across all epochs and SSPs. Similarly, some parts of the western coastal and central regions are noted as the hotspots of population exposure considering the hot-dry extremes.

Moreover, areas identified as hotspots owing to the rising population exposure from the hot-dry and hot-wet events may need more intervention in terms of climate change impact assessment followed by effective adaptation and mitigation planning. For instance, the Indo-Gangetic Plain of India is noted as a potential hotspot of population exposure to the compound extremes. It is one of the largest plains in the world, formed by multiple river systems, and it accommodates extensive agricultural activities. The said region is densely populated owing to favorable habitation conditions, including adequate surface and groundwater, suitable climatic conditions, and rich biodiversity. Nearly half of the total required food grains for 40% of the population of India is produced from this region solely (Pal et al. 2009). Furthermore, it plays a prominent role toward the food production of the entire South Asia region (Singh and Sontakke 2002). Therefore, future increases in the compound extremes and the associated rise in population exposure can substantially affect agricultural production and other socioeconomic activities over the Indo-Gangetic Plain (Jha et al. 2022). This, in consequence, can affect other South Asia regions also in terms of future food security.

To distinguish the relative contribution of climate and population toward the increasing future population exposure to the compound extremes, the total change in exposure is presented in terms of its three components, namely, climate influence, population influence, and their combined influence (as discussed in section 2b). Furthermore, climate extremes can pose more adverse societal consequences over densely populated regions as compared with sparsely populated regions. In this regard, four categories of populated regions (based on the population strength in 2020), i.e., low, moderate, high, and very high, are considered across India. Further, the three components, climate influence, population influence, and combined

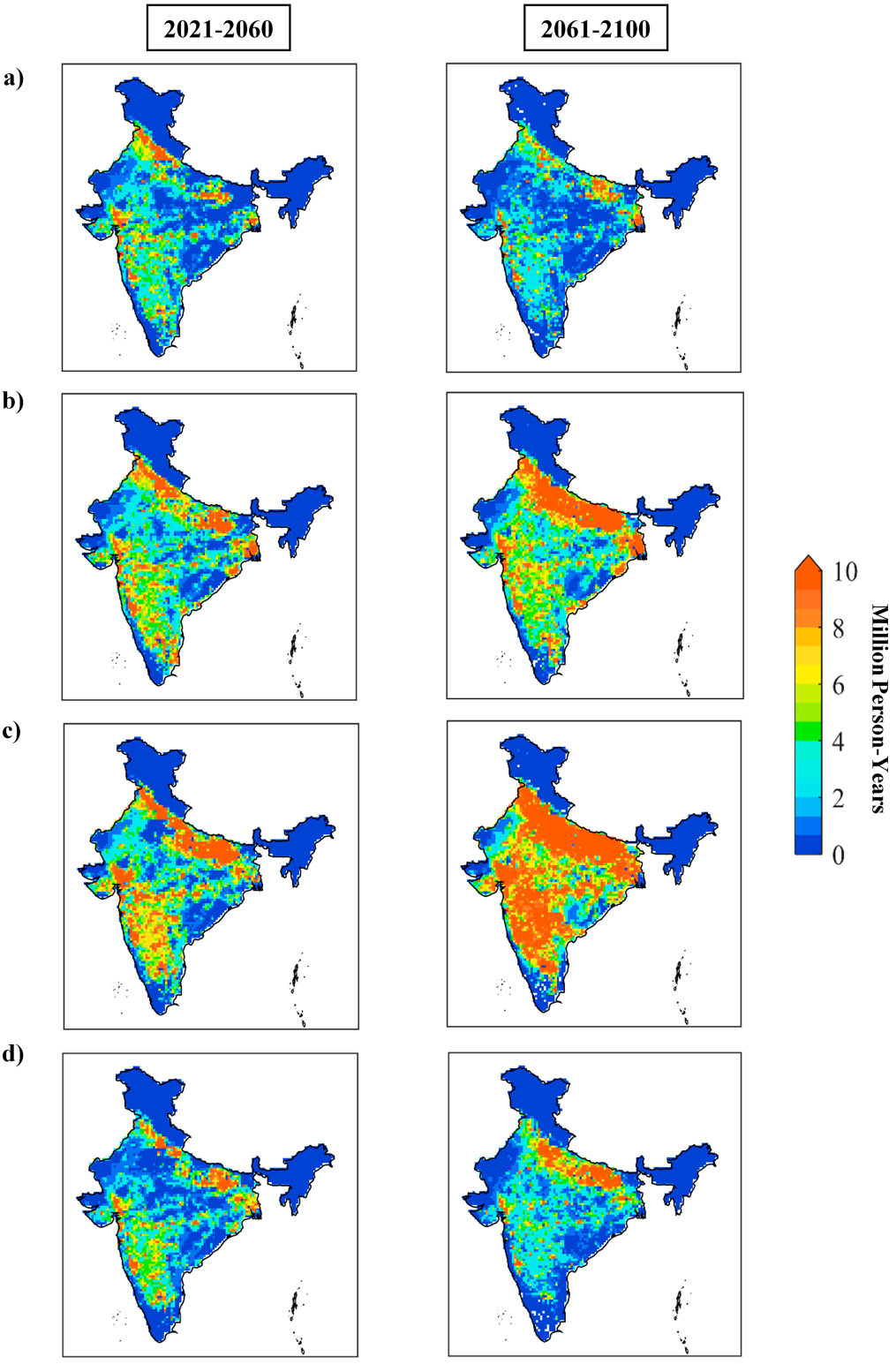

FIG. 7. Future changes in population exposure to the compound hot-dry extremes, expressed in person-years, for (left) near-future (2021–60) and (right) far-future (2061–2100) periods, considering four SSPs: (a) SSP1-2.6, (b) SSP2-4.5, (c) SSP3-7.0, and (d) SSP5-8.5, across India.

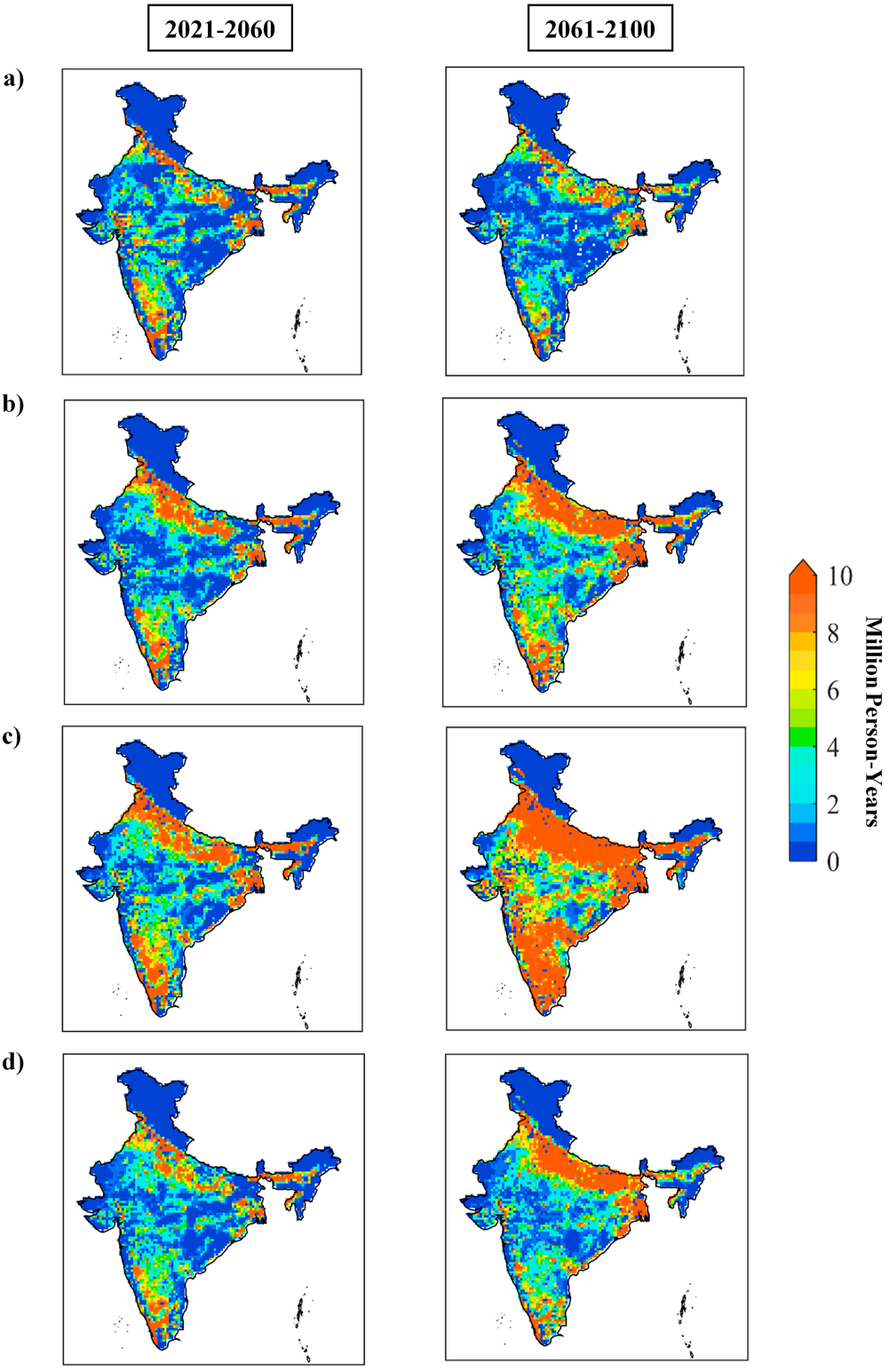

FIG. 8. As in Fig. 7, but for hot-wet compound extremes.

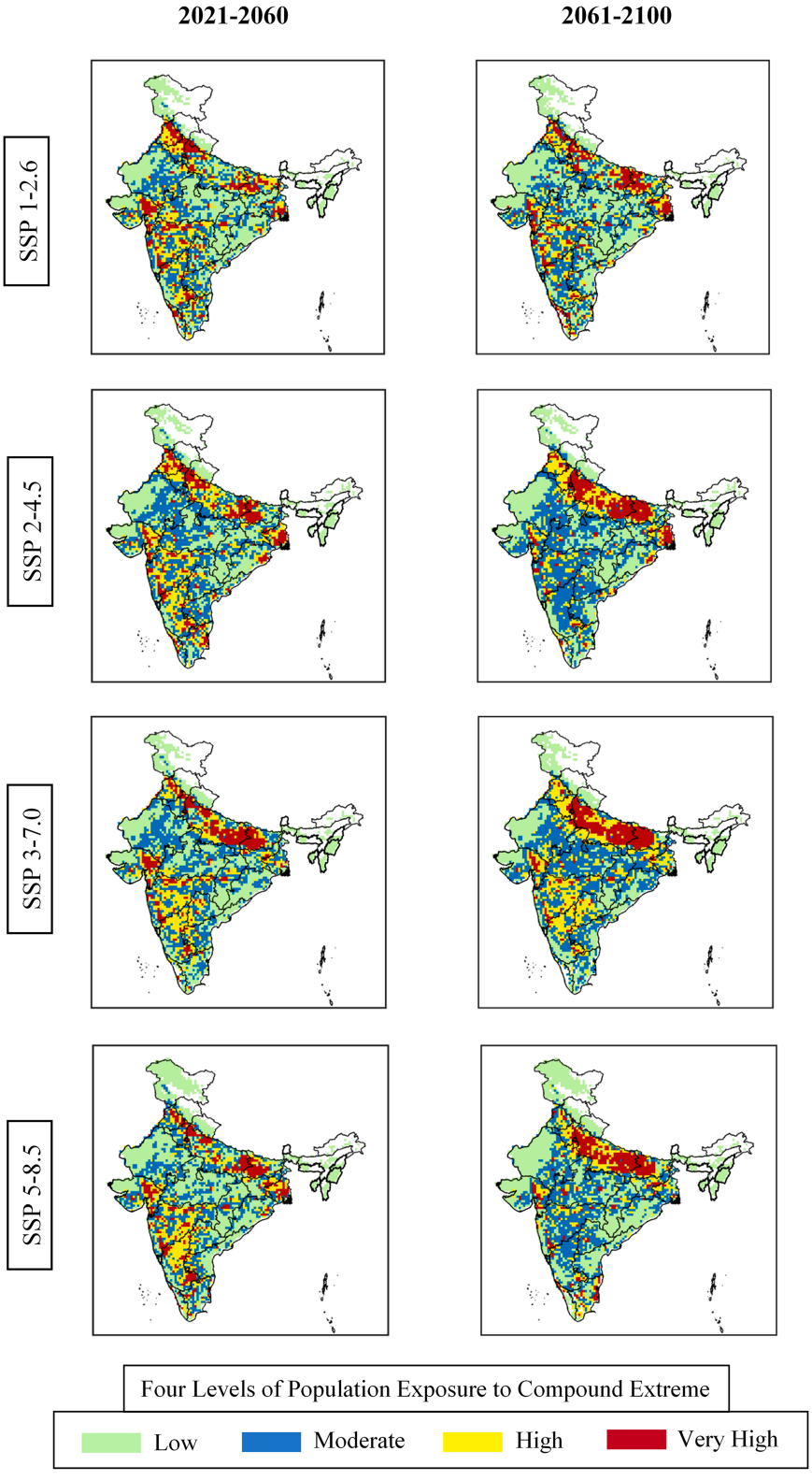

FIG. 9. Future hotspots identified on the basis of the projected change in the population exposure to hot-dry extremes considering the historical (1981–2020) and future periods [near future (2021–60) and far future (2061–2100)], for four SSPs: SSP1-2.6, SSP2-4.5, SSP3-7.0, and SSP5-8.5.

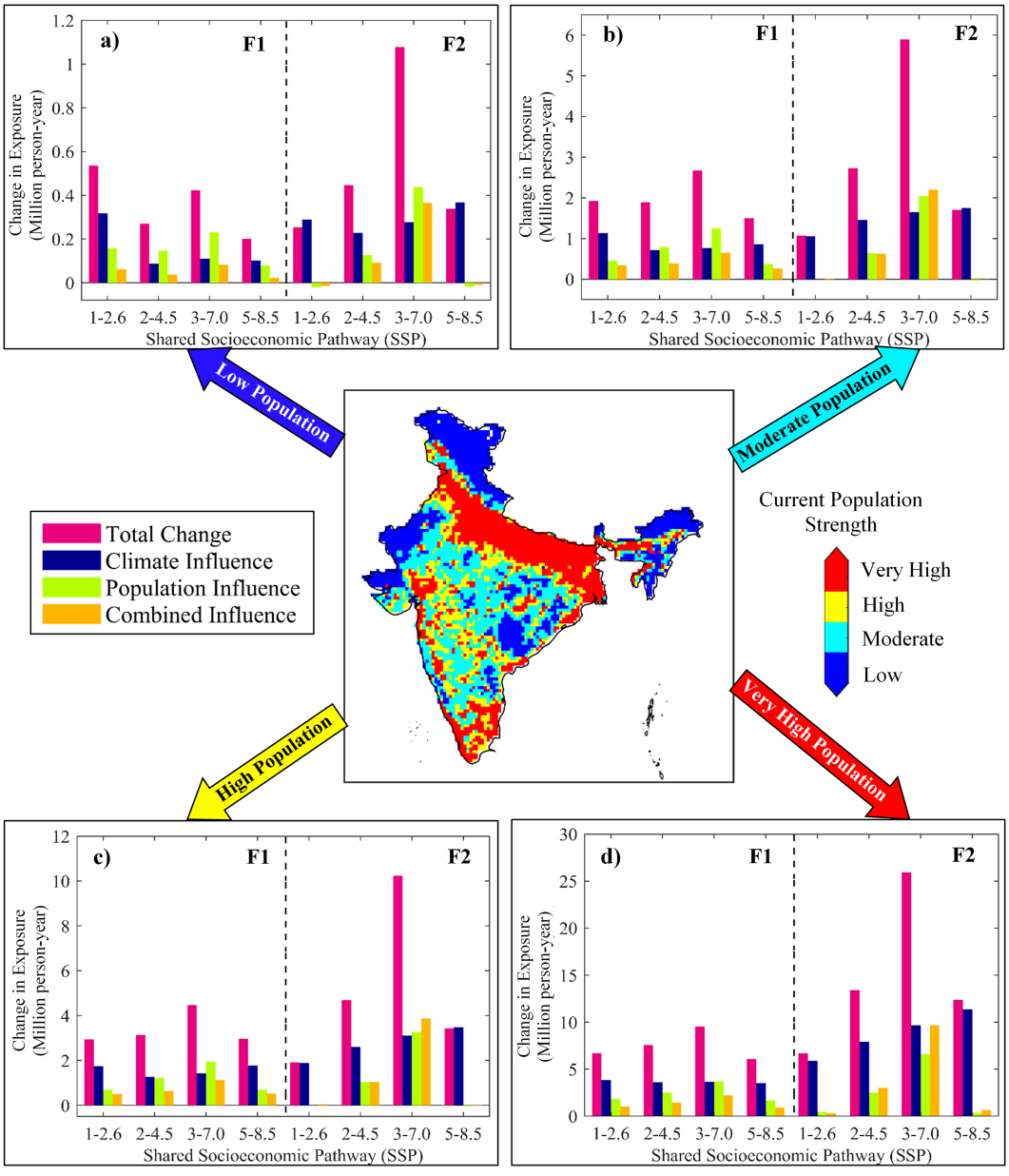

FIG. 10. Decomposition of the contribution from climate influence, population influence, and combined influence toward the total projected change in population exposure to compound hot-wet extreme under four SSPs: SSP1-2.6, SSP2-4.5, SSP3-7.0, and SSP5-8.5, over the four categories of populated regions based on the current (in the year 2020) population strength, i.e., (a) low, (b) moderate, (c) high, and (d) very high. The first half of each bar plot in (a)–(d) up to the vertical dashed dividing line shows results corresponding to near-future (F1: 2021–60), and the next half of the bar plot shows results for far-future (F2: 2061–2100) time periods.

influence, are evaluated separately for the low, moderate, high, and very high populated regions. Figure 10 (hot-wet extreme), along with Fig. S9 in the online supplemental material (hot-dry extreme), illustrate the decomposed contributions from the three components along with the total change for the four regions considering all the four SSPs during F1 and F2. The influence of the three contributing factors on increasing the population exposure to compound extremes varies based on the type of compound extreme, SSPs, future time epochs, and regions. In general, the potential future population exposure to hot-wet extremes is primarily influenced by the climate change factor, while the population change largely drives the exposure to hot-dry extremes. For instance, across the densely populated areas, the dominant factor driving the rise in overall exposure to the hot-wet extremes is the climate change influence, consistent across all four SSPs. Additionally, when considering all four regions, the same is noticed under SSP1 and SSP5 during both the future periods. Considering both hot-wet and hot-dry extremes,

the influence of climate is identified as the predominant factor during the far future period, for majority of the regions and SSPs, with the exception of SSP3. This emphasizes the crucial role that future climate change plays in amplifying the population exposure to compound extremes in a warmer future. On the contrary, the predominant influence on increasing overall population exposure to hot-dry extremes is attributed to future changes in population under SSP3. Furthermore, the maximum increase in the total population exposure to both hot-dry and hot-wet extremes is noted during F2 under SSP3 across all four regions, wherein the exposure to hot-wet extremes is dominated by the combined influence from climate change and population change. This indicates that the combined effects of population increase and climate change can induce more risks of population exposure. In general, a relatively greater increase in the exposure is found in the SSP3 scenario for all the regions and time periods, followed by SSP2, SSP5, and SSP1. As SSP3 is a high population growth scenario (Jones and O'Neill 2016), the future population influence is higher in SSP3 across all four regions, which contributes toward a relatively higher increase in the combined influence and the total exposure in consequence as compared with the other SSPs. Further, SSP2 represents a moderate population growth scenario; the worst climate change scenario, SSP5, assumes low population growth; SSP1 is also driven by slow population growth. Like SSP3, the relative increase in population under SSP2, SSP5, and SSP1 also follows the scenario based assumptions across all four regions. Further, a consistent increase in the total exposure is noticed from F1 to F2 in the case of SSP2 and SSP3 for both hot-dry and hot-wet extremes. However, a reduction in the total exposure is noted in F2 as of that in F1 under the SSP1 and SSP5 scenarios. The reduction in exposure mostly resulted from the projected decrease in population and combined influence. However, climate change exerts a greater effect on the exposure that offsets the negative contribution from population and results in increasing the total exposure. Consistent positive climate influence for hot-wet and hot-dry compound extremes indicates increase in the individual hot, dry, and wet extremes in the future, irrespective of the four SSPs, two epochs, and four regions. Previous studies reported higher increase in the frequency of future hot extremes as compared with the precipitation extremes across many regions of the globe, including India (Li et al. 2021; Yaduvanshi et al. 2021). Thus, the increase in both the hot-wet and hot-dry compound extremes might be dominated by the projected hot extreme occurrences as compared with the wet/dry extremes. Unlike the low, moderate, and highly populated regions, the declining population and combined influence components in SSP1 and SSP5 during F2 are not evidenced in the very highly populated regions. It indicates that under all the socioeconomic development pathways, the densely populated regions in India are going to be more populated. Further, the projected increase in climate influence is also noted across all SSPs over the very highly populated regions. Because of this, the said regions of the country are noticed with considerably higher increase in population exposure considering both hot-wet and hot-dry extremes. Consequently, the densely populated regions at present are going to face enhanced societal vulnerability in future as compared with the relatively less populated regions. Furthermore, future increase in the exposure is expected to be more in the case of hot-wet extreme relative to the hot-dry extremes during the far future period across all SSPs and regions; however, during the near-future period, it varies across the regions, and future warming and socioeconomic development scenarios. For instance, under the worst climate change scenario SSP5, higher exposure level is noted from the hot-wet extremes in the densely populated regions, whereas, over the low and moderately populated regions, the same is noted for the hot-dry extremes.

In brief, increased future population exposure from the compound hot-dry and hot-wet extremes is associated with future climate change to a great extent. Additionally, highly populated regions in India are expected to experience more adversity due to the hot-wet extremes in the future as compared with the hot-dry extremes. More efforts to control future warming and increasing populations can lead to substantial societal impacts being avoided in the future.

4. Conclusions

Compound precipitation–temperature extremes are expected to be more frequent and intense in the future due to climate change under continuing warming conditions. India being a developing country with the largest population in the world, growing exposure from the aforementioned compound extremes can pose huge societal impacts in multiple ways. In this study, the temporal changes in the compound hot-dry and hot-wet events and their influence on population exposure are evaluated across India, considering both historical and future time periods.

Recent decades (2001–20) have witnessed more frequent and spatially extensive hot-dry and hot-wet extremes as compared with the previous two time epochs (1951–80 and 1981–2000). However, the historical increases in population exposure to the hot-wet extreme have more prominence as compared with the hot-dry events across the country. To estimate the expected future changes in population exposure, the climate and population projections are utilized under four Shared Socioeconomic Pathways (SSPs), i.e., SSP1-2.6, SSP2-4.5, SSP3-7.0, and SSP5-8.5. Our study indicates an increase of more than 10 million person-year exposure (over $0.25° \times 0.25°$ grid) from the compound extremes across many regions of the country under the worst climate change scenario, i.e., SSP5-8.5. Under a moderate scenario, e.g., SSP3-7.0, the maximum extent of spatial coverage is noticed with higher exposure and the least in the case of SSP1-2.6. This can be attributed to the larger population increase in SSP3-7.0, which represents the high population growth scenario among the four SSPs. The Indo-Gangetic Plain and southernmost coastal (western-coastal and central) regions are found to be the future hotspots with the maximum increase in exposure to hot-wet (hot-dry) extremes under all the projected warming and population scenarios. Further, the contribution from climate, population, and their combined influence toward the expected exposure increase are assessed over the four categories of populated regions (i.e., low, moderate, high, and very high populated regions) based on the current population strength.

Our study further indicates that climate change factor is going to contribute the most toward the exposure increase to hot-wet extremes in comparison with the other two factors, i.e., change in population and combined change in both population and climate characteristics in the future. However, the maximum increase in exposure for each of the four regions is dominated by the combined influence of climate and population. This indicates that the combined effects of population increase concurrent with climate change can induce more societal adversities. Reduced exposure is noticed under SSP1-2.6 and SSP 5-8.5, which mostly resulted from the projected decrease in population and combined influence during the far future period. The densely populated regions of the country at present are going to exhibit a considerably higher increase in future population exposure as compared with that of the low-populated regions. Furthermore, the highly populated regions will be more exposed to the hot-wet extremes in the future as compared with the hot-dry extremes. Understanding from this study can contribute to assessing climate change risks from the compound hydroclimatic extremes across India. Estimated future changes in population exposure across different regions from the hot-dry and hot-wet extremes can assist in reducing socioeconomic consequences in the future.

Last, the analysis and conclusions are based on the climate simulations obtained in the latest GCMs (under CMIP6). Further improvement in terms of quality and spatial resolution of the outputs will help us to get a better assessment. Projected population growth also holds uncertainty as it may differ from the real future growth owing to the assumption-based future socioeconomic developments, particularly in the indicated hotspot regions. Nonetheless, the results will definitely be helpful for adopting socioeconomic decisions toward the welfare of society.

Acknowledgments. The work was partially supported by the sponsored projects supported by Ministry of Earth Sciences (MoES), government of India, through a sponsored project. Author Rajib Maity acknowledges support from the Alexander von Humboldt-Stiftung/Foundation as a Humboldt Fellow. We acknowledge India Meteorological Department (IMD), NASA Center for Climate Simulations (NCCS-THREDDS), and NASA Socioeconomic Data and Applications Center (SEDAC) for the availability of the historical and future climate and population datasets.

Data availability statement. All of the datasets used in this study are freely accessible from various sources. Observed daily precipitation (https://www.imdpune.gov.in/cmpg/Griddata/Rainfall_25_NetCDF.html) and maximum temperature (https://www.imdpune.gov.in/cmpg/Griddata/Max_1_Bin.html) data for the Indian mainland are obtained from Climate Research and Services of India Meteorological Department (https://www.imdpune.gov.in/lrfindex.php). Future projections of the climate data are obtained from NASA Earth Exchange Global Daily Downscaled Projections (NEX-GDDP-CMIP6) archive (Thrasher et al. 2022) (https://www.nccs.nasa.gov/services/data-collections/land-based-products/nex-gddp-cmip6). Historical and future (Jones and O'Neill 2016) population data are collected from the NASA Socioeconomic Data and Applications Center (SEDAC) (https://sedac.ciesin.columbia.edu/data/sets/browse?facets=theme:population). The figures are created using MATLAB software (https://in.mathworks.com version R2022a).

REFERENCES

Adedeji, O., O. Reuben, and O. Olatoye, 2014: Global climate change. *J. Geosci. Environ. Prot.*, **2**, 114–122, https://doi.org/10.4236/gep.2014.22016.

Ali, H., and V. Mishra, 2018: Increase in subdaily precipitation extremes in India under 1.5 and 2.0°C warming worlds. *Geophys. Res. Lett.*, **45**, 6972–6982, https://doi.org/10.1029/2018GL078689.

Avashia, V., A. Garg, and H. Dholakia, 2021: Understanding temperature related health risk in context of urban land use changes. *Landscape Urban Plann.*, **212**, 104107, https://doi.org/10.1016/j.landurbplan.2021.104107.

Bandyopadhyay, N., C. Bhuiyan, and A. K. Saha, 2016: Heat waves, temperature extremes and their impacts on monsoon rainfall and meteorological drought in Gujarat, India. *Nat. Hazards*, **82**, 367–388, https://doi.org/10.1007/s11069-016-2205-4.

Breinl, K., G. Di Baldassarre, M. Mazzoleni, D. Lun, and G. Vico, 2020: Extreme dry and wet spells face changes in their duration and timing. *Environ. Res. Lett.*, **15**, 074040, https://doi.org/10.1088/1748-9326/ab7d05.

CIESIN, 2018a: Gridded Population of the World, Version 4 (GPWv4): Population Count, Revision 11. Center for International Earth Science Information Network, Columbia University, accessed June 2022, https://doi.org/10.7927/H45Q4T5F.

——, 2018b: Documentation for the Gridded Population of the World, version 4 (GPWv4), revision 11 data sets. Center for International Earth Science Information Network, Columbia University, 53 pp., https://doi.org/10.7927/H45Q4T5F.

Chen, R., H. Yan, F. Liu, W. Du, and Y. Yang, 2020: Multiple global population datasets: Differences and spatial distribution characteristics. *ISPRS Int. J. Geoinf.*, **9**, 637, https://doi.org/10.3390/ijgi9110637.

Cho, C., R. Li, S. Y. Wang, J. H. Yoon, and R. R. Gillies, 2016: Anthropogenic footprint of climate change in the June 2013 northern India flood. *Climate Dyn.*, **46**, 797–805, https://doi.org/10.1007/s00382-015-2613-2.

Cook, B. I., J. S. Mankin, K. Marvel, A. P. Williams, J. E. Smerdon, and K. J. Anchukaitis, 2020: Twenty-first century drought projections in the CMIP6 forcing scenarios. *Earth's Future*, **8**, e2019EF001461, https://doi.org/10.1029/2019EF001461.

CRED, 2023: Emergency Events Database (EM-DAT). Centre for Research on the Epidemiology of Disasters, accessed March 2023, https://public.emdat.be/data.

Dash, S., and R. Maity, 2019: Temporal evolution of precipitation-based climate change indices across India: Contrast between pre- and post-1975 features. *Theor. Appl. Climatol.*, **138**, 1667–1678, https://doi.org/10.1007/s00704-019-02923-8.

——, and ——, 2021: Revealing alarming changes in spatial coverage of joint hot and wet extremes across India. *Sci. Rep.*, **11**, 18031, https://doi.org/10.1038/s41598-021-97601-z.

——, and ——, 2023: Unfolding unique features of precipitation-temperature scaling across India. *Atmos. Res.*, **284**, 106601, https://doi.org/10.1016/j.atmosres.2022.106601.

De Luca, P., G. Messori, R. L. Wilby, M. Mazzoleni, and G. Di Baldassarre, 2020: Concurrent wet and dry hydrological extremes at the global scale. *Earth Syst. Dyn.*, **11**, 251–266, https://doi.org/10.5194/esd-11-251-2020.

Dhillon, A., 2019: India heatwave: Rain brings respite for some but death toll rises. *Guardian*, 17 June, https://www.theguardian.com/world/2019/jun/17/india-heatwave-rain-brings-respite-for-some-but-death-toll-rises.

Doxsey-Whitfield, E., K. MacManus, S. B. Adamo, L. Pistolesi, J. Squires, O. Borkovska, and S. R. Baptista, 2015: Taking advantage of the improved availability of census data: A first look at the gridded population of the world, version 4. *Pap. Appl. Geogr.*, **1**, 226–234, https://doi.org/10.1080/23754931.2015.1014272.

Fakhruddin, B. S. H. M., K. Boylan, A. Wild, and R. Robertson, 2019: Assessing vulnerability and risk of climate change. *Climate Extremes and their Implications for Impact and Risk Assessment*, J. Sillmann, S. Sippel, and S. Russo, Eds., Elsevier, 217–241, https://doi.org/10.1016/B978-0-12-814895-2.00012-4.

Ganguli, P., 2023: Amplified risk of compound heat stress-dry spells in urban India. *Climate Dyn.*, **60**, 1061–1078, https://doi.org/10.1007/s00382-022-06324-y.

Gao, Z., Y. Hou, and W. Chen, 2019: Enhanced sensitivity of the urban heat island effect to summer temperatures induced by urban expansion. *Environ. Res. Lett.*, **14**, 094005, https://doi.org/10.1088/1748-9326/ab2740.

Guntu, R. K., and A. Agarwal, 2021: Disentangling increasing compound extremes at regional scale during Indian summer monsoon. *Sci. Rep.*, **11**, 16447, https://doi.org/10.1038/s41598-021-95775-0.

Gupta, A. K., and S. Guleria, 2017: Heat Wave 2016, India: A documentation study (based on State of Telangana and Odisha status). Tech. Rep., 52 pp., https://doi.org/10.13140/RG.2.2.13035.23847.

Gupta, N., 2019: Monsoon in India: Floods leave nearly 200 dead in 4 states, Uttarakhand, Kashmir also hit. *India Today*, 13 August, https://www.indiatoday.in/india/story/monsoon-in-india-floods-leave-nearly-200-dead-in-4-states-uttarakhand-kashmir-also-hit-1580192-2019-08-12.

Hao, Z., T. J. Phillips, F. Hao, and X. Wu, 2019: Changes in the dependence between global precipitation and temperature from observations and model simulations. *Int. J. Climatol.*, **39**, 4895–4906, https://doi.org/10.1002/joc.6111.

Hu, J., Z. Yang, C. Hou, and W. Ouyang, 2023: Compound risk dynamics of drought by extreme precipitation and temperature events in a semi-arid watershed. *Atmos. Res.*, **281**, 106474, https://doi.org/10.1016/j.atmosres.2022.106474.

Iyakaremye, V., and Coauthors, 2021: Increased high-temperature extremes and associated population exposure in Africa by the mid-21st century. *Sci. Total Environ.*, **790**, 148162, https://doi.org/10.1016/j.scitotenv.2021.148162.

Jebeile, J., and M. Crucifix, 2020: Multi-model ensembles in climate science: Mathematical structures and expert judgements. *Stud. Hist. Philos. Sci.*, **83**, 44–52, https://doi.org/10.1016/j.shpsa.2020.03.001.

Jha, R., A. Mondal, A. Devanand, M. K. Roxy, and S. Ghosh, 2022: Limited influence of irrigation on pre-monsoon heat stress in the Indo-Gangetic Plain. *Nat. Commun.*, **13**, 4275, https://doi.org/10.1038/s41467-022-31962-5.

Jha, S., L. Gudmundsson, and S. I. Seneviratne, 2023: Partitioning the uncertainties in compound hot and dry precipitation, soil moisture, and runoff extremes projections in CMIP6. *Earth's Future*, **11**, e2022EF003315, https://doi.org/10.1029/2022EF003315.

Jones, B., 2014: Assessment of a gravity-based approach to constructing future spatial population scenarios. *J. Popul. Res.*, **31**, 71–95, https://doi.org/10.1007/s12546-013-9122-0.

——, and B. C. O'Neill, 2016: Spatially explicit global population scenarios consistent with the Shared Socioeconomic Pathways. *Environ. Res. Lett.*, **11**, 084003, https://doi.org/10.1088/1748-9326/11/8/084003.

——, ——, L. Mcdaniel, S. Mcginnis, L. O. Mearns, and C. Tebaldi, 2015: Future population exposure to US heat extremes. *Nat. Climate Change*, **5**, 652–655, https://doi.org/10.1038/nclimate2631.

Jose, D. M., A. M. Vincent, and G. S. Dwarakish, 2022: Improving multiple model ensemble predictions of daily precipitation and temperature through machine learning techniques. *Sci. Rep.*, **12**, 4678, https://doi.org/10.1038/s41598-022-08786-w.

Kansal, M. L., and S. Singh, 2022: Flood management issues in hilly regions of Uttarakhand (India) under changing climatic conditions. *Water*, **14**, 1879, https://doi.org/10.3390/w14121879.

Katzenberger, A., J. Schewe, J. Pongratz, and A. Levermann, 2021: Robust increase of Indian monsoon rainfall and its variability under future warming in CMIP6 models. *Earth Syst. Dyn.*, **12**, 367–386, https://doi.org/10.5194/esd-12-367-2021.

Knowlton, K., and Coauthors, 2014: Development and implementation of South Asia's first heat-health action plan in Ahmedabad (Gujarat, India). *Int. J. Environ. Res. Public Health*, **11**, 3473–3492, https://doi.org/10.3390/ijerph110403473.

Kumar, P., J. Tokas, N. Kumar, M. Lal, H. Singal, and C. Praveen Kumar, 2018: Climate change consequences and its impact on agriculture and food security. *Int. J. Chem. Stud.*, **6**, 124–133.

Labonte, M.-P., and T. M. Merlis, 2023: Evaluation of changes in dry and wet precipitation extremes in warmer climates using a passive water vapor modelling approach. *J. Climate*, **36**, 2167–2182, https://doi.org/10.1175/JCLI-D-22-0048.1.

Lane, K., K. Charles-Guzman, K. Wheeler, Z. Abid, N. Graber, and T. Matte, 2013: Health effects of coastal storms and flooding in urban areas: A review and vulnerability assessment. *J. Environ. Public Health*, **2013**, 913064, https://doi.org/10.1155/2013/913064.

Li, C., F. Zwiers, X. Zhang, G. Li, Y. Sun, and M. Wehner, 2021: Changes in annual extremes of daily temperature and precipitation in CMIP6 models. *J. Climate*, **34**, 3441–3460, https://doi.org/10.1175/JCLI-D-19-1013.1.

Maity, R., 2022: *Statistical Methods in Hydrology and Hydroclimatology*. 2nd ed. Springer, 436 pp., https://doi.org/10.1007/978-981-16-5517-3.

——, and D. N. Kumar, 2008: Probabilistic prediction of hydroclimatic variables with nonparametric quantification of uncertainty. *J. Geophys. Res.*, **113**, D14105, https://doi.org/10.1029/2008JD009856.

Mall, R. K., R. K. Srivastava, T. Banerjee, O. P. Mishra, D. Bhatt, and G. Sonkar, 2019: Disaster risk reduction including climate change adaptation over South Asia: Challenges and ways forward. *Int. J. Disaster Risk Sci.*, **10**, 14–27, https://doi.org/10.1007/s13753-018-0210-9.

Mazdiyasni, O., and Coauthors, 2017: Increasing probability of mortality during Indian heat waves. *Sci. Adv.*, **3**, e1700066, https://doi.org/10.1126/sciadv.1700066.

Meng, Y., Z. Hao, S. Feng, X. Zhang, and F. Hao, 2022: Increase in compound dry-warm and wet-warm events under global warming in CMIP6 models. *Global Planet. Change*, **210**, 103773, https://doi.org/10.1016/j.gloplacha.2022.103773.

Mishra, A., and S. C. Liu, 2014: Changes in precipitation pattern and risk of drought over India in the context of global warming. *J. Geophys. Res. Atmos.*, **119**, 7833–7841, https://doi.org/10.1002/2014JD021471.

Mishra, V., R. Shah, and B. Thrasher, 2014: Soil moisture droughts under the retrospective and projected climate in India. *J. Hydrometeor.*, **15**, 2267–2292, https://doi.org/10.1175/JHM-D-13-0177.1.

——, K. Thirumalai, D. Singh, and S. Aadhar, 2020: Future exacerbation of hot and dry summer monsoon extremes in India. *npj Climate Atmos. Sci.*, **3**, 10, https://doi.org/10.1038/s41612-020-0113-5.

——, A. D. Tiwari, and R. Kumar, 2022: Warming climate and ENSO variability enhance the risk of sequential extremes in India. *One Earth*, **5**, 1250–1259, https://doi.org/10.1016/j.oneear.2022.10.013.

Mitra, A., 2021: A comparative study on the skill of CMIP6 models to preserve daily spatial patterns of monsoon rainfall over India. *Front. Climate*, **3**, 654763, https://doi.org/10.3389/fclim.2021.654763.

Mukherjee, S., and V. Mishra, 2018: A sixfold rise in concurrent day and night-time heatwaves in India under 2°C warming. *Sci. Rep.*, **8**, 16922, https://doi.org/10.1038/s41598-018-35348-w.

——, S. Aadhar, D. Stone, and V. Mishra, 2018: Increase in extreme precipitation events under anthropogenic warming in India. *Wea. Climate Extremes*, **20**, 45–53, https://doi.org/10.1016/j.wace.2018.03.005.

Murali, G., T. Iwamura, S. Meiri, and U. Roll, 2023: Future temperature extremes threaten land vertebrates. *Nature*, **615**, 461–467, https://doi.org/10.1038/s41586-022-05606-z.

Myhre, G., and Coauthors, 2019: Frequency of extreme precipitation increases extensively with event rareness under global warming. *Sci. Rep.*, **9**, 16063, https://doi.org/10.1038/s41598-019-52277-4.

Nayak, G., K. K. Sardar, B. C. Das, and D. Das, Eds., 2022: *Impact of Climate Change on Livestock Health and Production*. CRC Press, 314 pp.

Pai, D. S., S. A. Nair, and A. N. Ramanathan, 2013: Long term climatology and trends of heat waves over India during the recent 50 years (1961-2010). *Mausam*, **64**, 585–604, https://doi.org/10.54302/mausam.v64i4.742.

——, L. Sridhar, M. R. Badwaik, and M. Rajeevan, 2015: Analysis of the daily rainfall events over India using a new long period (1901–2010) high resolution (0.25° × 0.25°) gridded rainfall data set. *Climate Dyn.*, **45**, 755–776, https://doi.org/10.1007/s00382-014-2307-1.

Pal, D. K., T. Bhattacharyya, P. Srivastava, P. Chandran, and S. K. Ray, 2009: Soils of the Indo-Gangetic Plains: Their historical perspective and management. *Curr. Sci.*, **96**, 1193–1202.

Park, T., H. Hashimoto, W. Wang, B. Thrasher, A. R. Michaelis, T. Lee, I. G. Brosnan, and R. R. Nemani, 2022: What does global land climate look like at 2°C warming? *Earth's Future*, **11**, e2022EF003330, https://doi.org/10.1029/2022EF003330.

Pattanayak, S., R. S. Nanjundiah, and D. N. Kumar, 2017: Linkage between global sea surface temperature and hydroclimatology of a major river basin of India before and after 1980. *Environ. Res. Lett.*, **12**, 124002, https://doi.org/10.1088/1748-9326/aa9664.

Pielke, R. A., 2005: Misdefining "climate change": Consequences for science and action. *Environ. Sci. Policy*, **8**, 548–561, https://doi.org/10.1016/j.envsci.2005.06.013.

Pradhan, B., T. Kjellstrom, D. Atar, P. Sharma, B. Kayastha, G. Bhandari, and P. K. Pradhan, 2019: Heat stress impacts on cardiac mortality in Nepali migrant workers in Qatar. *Cardiology*, **143**, 37–48, https://doi.org/10.1159/000500853.

Prakash, S., and Coauthors, 2015: Seasonal intercomparison of observational rainfall datasets over India during the southwest monsoon season. *Int. J. Climatol.*, **35**, 2326–2338, https://doi.org/10.1002/joc.4129.

Rajeev, A., S. S. Mahto, and V. Mishra, 2022: Climate warming and summer monsoon breaks drive compound dry and hot extremes in India. *iScience*, **25**, 105377, https://doi.org/10.1016/j.isci.2022.105377.

Ray, K., P. Pandey, C. Pandey, A. P. Dimri, and K. Kishore, 2019: On the recent floods in India. *Curr. Sci.*, **117**, 204–218, https://doi.org/10.18520/cs/v117/i2/204-218.

Raza, A., A. Razzaq, S. S. Mehmood, X. Zou, X. Zhang, Y. Lv, and J. Xu, 2019: Impact of climate change on crops adaptation and strategies to tackle its outcome: A review. *Plants*, **8**, 34, https://doi.org/10.3390/plants8020034.

Ridha, T., A. D. Ross, and A. Mostafavi, 2022: Climate change impacts on infrastructure: Flood risk perceptions and evaluations of water systems in coastal urban areas *Int. J. Disaster Risk Reduct.*, **73**, 102883, https://doi.org/10.1016/j.ijdrr.2022.102883.

Roderick, T. P., and C. Wasko, 2020: An improved covariate for projecting future rainfall extremes? *Water Resour. Res.*, **56**, e2019WR026924, https://doi.org/10.1029/2019WR026924.

Rogers, C. D. W., M. Ting, C. Li, K. Kornhuber, E. D. Coffel, R. M. Horton, C. Raymond, and D. Singh, 2021: Recent increases in exposure to extreme humid-heat events disproportionately affect populated regions. *Geophys. Res. Lett.*, **48**, e2021GL094183, https://doi.org/10.1029/2021GL094183.

Rohini, P., M. Rajeevan, and A. K. Srivastava, 2016: On the variability and increasing trends of heat waves over India. *Sci. Rep.*, **6**, 26153, https://doi.org/10.1038/srep26153.

Ross, R. S., T. N. Krishnamurti, S. Pattnaik, and D. S. Pai, 2018: Decadal surface temperature trends in India based on a new high-resolution data set. *Sci. Rep.*, **8**, 7452, https://doi.org/10.1038/s41598-018-25347-2.

Sahana, A. S., S. Ghosh, A. Ganguly, and R. Murtugudde, 2015: Shift in Indian summer monsoon onset during 1976/1977. *Environ. Res. Lett.*, **10**, 054006, https://doi.org/10.1088/1748-9326/10/5/054006.

Salvadori, G., and C. De Michele, 2004: Frequency analysis via copulas: Theoretical aspects and applications to hydrological events. *Water Resour. Res.*, **40**, W12511, https://doi.org/10.1029/2004WR003133.

Sara, H., G. Patrick, and W. John, 2023: India overtakes China as the world's most populous country. World Population Prospects 2022: Summary of Results. UN DESA/POP/2022/TR/NO.3, 5 pp., https://www.un.org/development/desa/dpad/wp-content/uploads/sites/45/PB153.pdf.

Sarkar, S., and R. Maity, 2020: Increase in probable maximum precipitation in a changing climate over India. *J. Hydrol.*, **585**, 124806, https://doi.org/10.1016/j.jhydrol.2020.124806.

Schewe, J., and Coauthors, 2014: Multimodel assessment of water scarcity under climate change. *Proc. Natl. Acad. Sci. USA*, **111**, 3245–3250, https://doi.org/10.1073/pnas.1222460110.

Seneviratne, S. I., N. Nicholls, and D. Easterling, 2012: Changes in climate extremes and their impacts on the natural physical environment. *Managing the Risks of Extreme Events and Disasters to Advance Climate Change Adaptation*, C. B. Field et al., Eds., Cambridge University Press, 109–230.

Serinaldi, F., B. Bonaccorso, A. Cancelliere, and S. Grimaldi, 2009: Probabilistic characterization of drought properties through copulas. *Phys. Chem. Earth Parts ABC*, **34**, 596–605, https://doi.org/10.1016/j.pce.2008.09.004.

Sharma, S., and P. P. Mujumdar, 2019: On the relationship of daily rainfall extremes and local mean temperature. *J. Hydrol.*, **572**, 179–191, https://doi.org/10.1016/j.jhydrol.2019.02.048.

Shen, M., W. Huang, M. Chen, B. Song, G. Zeng, and Y. Zhang, 2020: (Micro) plastic crisis: Un-ignorable contribution to global greenhouse gas emissions and climate change. *J. Clean. Prod.*, **254**, 120138, https://doi.org/10.1016/j.jclepro.2020.120138.

Shepard, D., 1968: Two-dimensional interpolation function for irregularly-spaced data. *ACM'68: Proc. 1968 23rd ACM National Conference*, Association for Computing Machinery, 517–524, https://doi.org/10.1145/800186.810616.

Shrestha, S., T. Yao, and T. R. Adhikari, 2019: Analysis of rainfall trends of two complex mountain river basins on the southern slopes of the Central Himalayas. *Atmos. Res.*, **215**, 99–115, https://doi.org/10.1016/j.atmosres.2018.08.027.

Singh, D., M. Tsiang, B. Rajaratnam, and N. S. Diffenbaugh, 2014: Observed changes in extreme wet and dry spells during the south Asian summer monsoon season. *Nat. Climate Change*, **4**, 456–461, https://doi.org/10.1038/nclimate2208.

Singh, N., and N. A. Sontakke, 2002: On climatic fluctuations and environmental changes of the Indo-Gangetic Plains, India. *Climatic Change*, **52**, 287–313, https://doi.org/10.1023/A:1013772505484.

Singh, S., R. K. Mall, and N. Singh, 2021: Changing spatio-temporal trends of heat wave and severe heat wave events over India: An emerging health hazard. *Int. J. Climatol.*, **41**, E1831–E1845, https://doi.org/10.1002/joc.6814.

Srivastava, A. K., M. Rajeevan, and S. Kshirsagar, 2009: Development of a high resolution daily gridded temperature data set (1969–2005) for the Indian region. *Atmos. Sci. Lett.*, **10**, 249–254, https://doi.org/10.1002/asl.232.

Stevenson, S., S. Coats, D. Touma, J. Cole, F. Lehner, J. Fasullo, and B. Otto-Bliesner, 2022: Twenty-first century hydroclimate: A continually changing baseline, with more frequent extremes. *Proc. Natl. Acad. Sci. USA*, **119**, e2108124119, https://doi.org/10.1073/pnas.2108124119.

Stewart, J. Q., 1942: A measure of the influence of a population at a distance. *Sociometry*, **5**, 63–71, https://doi.org/10.2307/2784954.

Sun, S., T. L. Dai, Z. Y. Wang, J. M. Chou, Q. C. Chao, and P. J. Shi, 2021: Projected increases in population exposure of daily climate extremes in eastern China by 2050. *Adv. Climate Change Res.*, **12**, 804–813, https://doi.org/10.1016/j.accre.2021.09.014.

Tabari, H., S. Marofi, and M. Ahmadi, 2011: Long-term variations of water quality parameters in the Maroon River, Iran. *Environ. Monit. Assess.*, **177**, 273–287, https://doi.org/10.1007/s10661-010-1633-y.

Tegegne, G., Y. O. Kim, and J. K. Lee, 2019: Spatiotemporal reliability ensemble averaging of multimodel simulations. *Geophys. Res. Lett.*, **46**, 12 321–12 330, https://doi.org/10.1029/2019GL083053.

Thakur, R., and V. L. Manekar, 2022: Ranking of CMIP6 based high-resolution global climate models for India using TOPSIS. *ISH J. Hydraul. Eng.*, **29**, 175–188, https://doi.org/10.1080/09715010.2021.2015462.

Thrasher, B., W. Wang, A. Michaelis, F. Melton, T. Lee, and R. Nemani, 2022: NASA global daily downscaled projections, CMIP6. *Sci. Data*, **9**, 262, https://doi.org/10.1038/s41597-022-01393-4.

Tuholske, C., K. Caylor, C. Funk, A. Verdin, S. Sweeney, K. Grace, P. Peterson, and T. Evans, 2021: Global urban population exposure to extreme heat. *Proc. Natl. Acad. Sci. USA*, **118**, e2024792118, https://doi.org/10.1073/pnas.2024792118.

Varga, A., 2021: Climate change and its impact on agriculture. *Acta Hortic. Regiotecturae*, **24**, 50–57, https://doi.org/10.2478/ahr-2021-0010.

Wang, H. M., J. Chen, C. Y. Xu, J. Zhang, and H. Chen, 2020: A framework to quantify the uncertainty contribution of GCMs over multiple sources in hydrological impacts of climate change. *Earth's Future*, **8**, e2020EF001602, https://doi.org/10.1029/2020EF001602.

Wang, M., X. Fu, D. Zhang, F. Chen, M. Liu, S. Zhou, J. Su, and S. K. Tan, 2023: Assessing urban flooding risk in response to climate change and urbanization based on shared socioeconomic pathways. *Sci. Total Environ.*, **880**, 163470, https://doi.org/10.1016/j.scitotenv.2023.163470.

Wiréhn, L., Å. Danielsson, and T. S. S. Neset, 2015: Assessment of composite index methods for agricultural vulnerability to climate change. *J. Environ. Manage.*, **156**, 70–80, https://doi.org/10.1016/j.jenvman.2015.03.020.

WMO, 2020: WMO Statement on the State of the Global Climate in 2019. WMO-1248, 44 pp., https://library.wmo.int/idurl/4/56228.

Yaduvanshi, A., R. Bendapudi, T. Nkemelang, and M. New, 2021: Temperature and rainfall extremes change under current and future warming global warming levels across Indian climate zones. *Wea. Climate Extremes*, **31**, 100291, https://doi.org/10.1016/j.wace.2020.100291.

Yang, J., and Coauthors, 2021: Projecting heat-related excess mortality under climate change scenarios in China. *Nat. Commun.*, **12**, 1039, https://doi.org/10.1038/s41467-021-21305-1.

Yin, J., L. Slater, L. Gu, Z. Liao, S. Guo, and P. Gentine, 2022: Global increases in lethal compound heat stress: Hydrological drought hazards under climate change. *Geophys. Res. Lett.*, **49**, e2022GL100880, https://doi.org/10.1029/2022GL100880.

Zhang, P., O. Deschenes, K. Meng, and J. Zhang, 2018: Temperature effects on productivity and factor reallocation: Evidence from a half million Chinese manufacturing plants. *J. Environ. Econ. Manage.*, **88**, 1–17, https://doi.org/10.1016/j.jeem.2017.11.001.

Zhang, Y., Q. You, S. Ullah, C. Chen, L. Shen, and Z. Liu, 2023: Substantial increase in abrupt shifts between drought and flood events in China based on observations and model simulations. *Sci. Total Environ.*, **876**, 162822, https://doi.org/10.1016/j.scitotenv.2023.162822.

Zscheischler, J., and Coauthors, 2018: Future climate risk from compound events. *Nat. Climate Change*, **8**, 469–477, https://doi.org/10.1038/s41558-018-0156-3.